AD_____

Award Number: DAMD17-98-1-8325

TITLE: Cell Migration as a Therapeutic Target in Malignant Breast Cancer

PRINCIPAL INVESTIGATOR: George E. Plopper, Jr., Ph.D.

CONTRACTING ORGANIZATION: University of Nevada, Las Vegas
Las Vegas, Nevada 89154-1037

REPORT DATE: September 2000

TYPE OF REPORT: Annual Summary

PREPARED FOR: U.S. Army Medical Research and Materiel Command
Fort Detrick, Maryland 21702-5012

DISTRIBUTION STATEMENT: Approved for Public Release;
Distribution Unlimited

The views, opinions and/or findings contained in this report are those of the author(s) and should not be construed as an official Department of the Army position, policy or decision unless so designated by other documentation.

REPORT DOCUMENTATION PAGE

Form Approved
OMB No. 074-0188

1. AGENCY USE ONLY (Leave blank)	2. REPORT DATE	3. REPORT TYPE AND DATES COVERED
	September 2000	Annual Summary (1 Sep 99 - 31 Aug 00)

4. TITLE AND SUBTITLE
Cell Migration as a Therapeutic Target in Malignant Breast Cancer

5. FUNDING NUMBERS
DAMD17-98-1-8325

6. AUTHOR(S)
George E. Plopper, Jr., Ph.D.

7. PERFORMING ORGANIZATION NAME(S) AND ADDRESS(ES)
University of Nevada, Las Vegas
Las Vegas, Nevada 89154-1037

E-MAIL:
plopper@ccmail.nevada.edu

8. PERFORMING ORGANIZATION REPORT NUMBER

9. SPONSORING / MONITORING AGENCY NAME(S) AND ADDRESS(ES)
U.S. Army Research Office
P.O. Box 12211
Research Triangle park, NC 27709-2211

10. SPONSORING / MONITORING AGENCY REPORT NUMBER

11. SUPPLEMENTARY NOTES

12a. DISTRIBUTION / AVAILABILITY STATEMENT
Approved for public release; distribution unlimited

12b. DISTRIBUTION CODE

13. ABSTRACT ***(Maximum 200 Words)***

The object of this project is to develop a high-throughput method for screening potential inhibitors of breast cancer cell haptotaxis and chemotaxis, and to apply this method to identify signaling events mediating constitutive migration of malignant breast cells. The pathways that control these signaling events may be targets for development of new classes of anti-tumor drugs. The significant advances made during the second year of the project include the identification of three molecules that are involved in integrin-mediated cell signaling and migration (RACK1, Focal Adhesion Kinase, and Ca+2), the development of a model system for examining integrin-specific signaling in breast cells adhering to laminin-1, and the identification of perillyl alcohol as a non-cytotoxic inhibitor of breast cell migration.

14. SUBJECT TERMS	15. NUMBER OF PAGES
Breast Cancer, Extracellular Matrix, Integrins	69
	16. PRICE CODE

17. SECURITY CLASSIFICATION OF REPORT	18. SECURITY CLASSIFICATION OF THIS PAGE	19. SECURITY CLASSIFICATION OF ABSTRACT	20. LIMITATION OF ABSTRACT
Unclassified	Unclassified	Unclassified	Unlimited

NSN 7540-01-280-5500

Standard Form 298 (Rev. 2-89)
Prescribed by ANSI Std. Z39-18
298-102

FOREWORD

Opinions, interpretations, conclusions and recommendations are those of the author and are not necessarily endorsed by the U.S. Army.

___ Where copyrighted material is quoted, permission has been obtained to use such material.

___ Where material from documents designated for limited distribution is quoted, permission has been obtained to use the material.

___ Citations of commercial organizations and trade names in this report do not constitute an official Department of Army endorsement or approval of the products or services of these organizations.

__ In conducting research using animals, the investigator(s) adhered to the "Guide for the Care and Use of Laboratory Animals," prepared by the Committee on Care and use of Laboratory Animals of the Institute of Laboratory Resources, national Research Council (NIH Publication No. 86-23, Revised 1985).

__ For the protection of human subjects, the investigator(s) adhered to policies of applicable Federal Law 45 CFR 46.

_X_ In conducting research utilizing recombinant DNA technology, the investigator(s) adhered to current guidelines promulgated by the National Institutes of Health.

_X_ In the conduct of research utilizing recombinant DNA, the investigator(s) adhered to the NIH Guidelines for Research Involving Recombinant DNA Molecules.

N/A In the conduct of research involving hazardous organisms, the investigator(s) adhered to the CDC-NIH Guide for Biosafety in Microbiological and Biomedical Laboratories.

1/28/00

PI - Signature Date

Table of Contents

Introduction

The purpose of this project is to identify the mechanisms governing the constitutive migration of breast cancer cells, with an eye towards reducing the severity of malignant breast cancer by inhibiting the signaling pathways responsible for maintaining this migration. The approaches proposed in this project focus on developing an in vitro migration assay suitable for identifying new biochemical inhibitors of tumor cell migration, and on isolating a potentially novel integrin receptor that mediates constitutive migration of breast cancer cells on the extracellular matrix protein laminin-5. We have made substantial progress with regard to developing the migration assay but have abandoned the integrin isolation project, and have instead turned our attention to signaling activities of known proteins in human breast cells.

Body

The goals of this project have been defined in two specific aims. The progress in each Aim is described below.

Specific Aim 1: Define the components of the pertussis toxin-sensitive G protein signalling pathway that mediates migration of normal and malignant breast cells on laminin-5.

Specific elements of this aim that were to be addressed in the first 12 months of this project are:

Task 1. Optimize assays for identifying signalling proteins in migrating cells, Months 1-6.

In the course of developing a migration assay, we discovered that intracellular Ca^{+2} levels are directly proportional to migration rate in our cells, and that both of these factors vary considerably on different extracellular matrix proteins. We have focused our attention on following up on these findings.

a. Develop protein kinase and lipid kinase assays using whole cell lysates as starting material

RACK1: As previously reported in the 1999 annual report, we found that overexpression of the protein RACK1 inhibited migration of beast cells. Progress in this project was slowed by the fact that RACK1 overexpression appeared to be toxic to breast cells, so we abandoned the project. however, we did pursue the effects of RACK1 on migration of other cells that could express high levels of RACK1 (Chinese Hamster Ovary cells), and this resulted in submission of a manuscript characterizing RACK1 inhibition of migration. Though not directly related to breast cancer, it is a useful outcome of this work.

FAK/CAS: Laminin-5 is a heterotrimer composed of single α,β, and γ chains coiled together forming a characteristic cross-shaped structure. It is abundantly expressed in the basement of the breast epithelium where it plays a role in branching morphogenesis and adhesion and migration of breast cells. At present very little is known about the signals generated by laminin-5-binding integrins in breast cells, how this interaction controls cellular behavior, and what changes occur in these signaling pathways when breast cells undergo malignant transformation. We are investigating the role of focal adhesion kinase (FAK), a cytoplasmic protein tyrosine kinase, in controlling cell migration on laminin-5. FAK is an attractive candidate for analysis as it has been shown to be an important mediator of cell migration in a number of systems. The vast majority of studies on FAK and cell migration have occurred in systems that involve ECM substrates that contain Arg-Gly-Asp (RGD) integrin binding domains (fibronectin and vitronectin), such that very little is known about

FAK signaling through non-RGD substrates such as laminin-5 and their associated receptors (such as $\alpha 3\beta 1$ integrin). Almost nothing has been reported about FAK signaling in breast cancer, other than that it is overexpressed in malignant cells. Also, the contribution of FAK to signals generated by binding distinct forms of the same ECM molecules via the same integrin receptor has not been studied previously.

Our work has shown that malignant breast cells can be functionally distinguished from normal and immortalized cells by their ability to migrate constitutively on laminin-5. Importantly, inactivation of tyrosine kinases with the drug genistein inhibits integrin antibody-stimulated migration on laminin-5 in immortalized cells, and constitutive migration in malignant cells, suggesting that tyrosine kinases such as FAK may contribute to the TS2/16-mediated cAMP signaling response, and hence may be involved in controlling migration in normal and malignant cells. Preliminary data shows that FAK is activated when these cells adhere to laminin-5 (Figure 1).

A second means of stimulating migration on laminin-5 is through proteolytic cleavage of laminin-5 subunits. Recently, it was reported that specific proteolytic cleavage of the laminin-5 $\gamma 2$ chain by matrix metalloprotease-2 or elastase induces migration of breast epithelial cells through the $\alpha 3\beta 1$ integrin receptor. We have confirmed these findings in our lab (Figures 2 and 3). Furthermore, the cleaved form of laminin-5 is enriched in breast tumors and sites of active tissue remodeling, including mammary tissue from pregnant rats. Thus, in breast cells, the same integrin receptor, $\alpha 3\beta 1$, changes its migration signaling activity depending on the form of laminin-5 to which it binds. This is a relatively new area of integrin signaling research, and the molecular mechanisms that govern it are almost entirely unknown.

Proteolytic cleavage of laminin-5 appears to have the same effect on migration as addition of TS2/16, suggesting that the processing of laminin-5 may be the physiologically relevant equivalent of antibody-induced integrin activation. A major goal of this project is to test this hypothesis by comparing the signaling stimulated in each system.

To facilitate these studies we are constructing recombinant laminin-5 $\gamma 2$ chains that can be over-expressed in a tissue culture system. Figure 4A depicts the structure of wild-type laminin-5 with a $\gamma 2$ chain containing a $(Histidine)_6$-tag at the carboxyl terminus. A truncated version of the $\gamma 2$ chain, with a deletion of all amino acid residues amino terminal to the site of elastase cleavage, is also being constructed (Figure 4B). These constructs will allow us to compare laminin-5 signaling activity in a direct and controlled system.

HETEROTRIMERIC G PROTEINS: As reported in the 1999 annual report, we obtained cDNA constructs containing pertussis toxin-sensitive and –insensitive isoforms of $G\alpha$ subunits, and attempted to transfect them into our cells. This work has not progressed, for two main reasons: (1) Many of the cDNA constructs we received did not contain the G protein constructs we asked for, and repeated attempts to obtain these constructs from our collaborator have failed; (2) We submitted a manuscript describing the original findings that formed the basis for this project, and it was rejected by two different journals. Thus our focus has been on shoring up the original findings before proceeding with this project.

b. Optimize methods for isolating integrin complexes

Progress: This project was abandoned after the first year.

c. Optimize sensitivity and throughput of non-fluorescence, dye-based cell migration assay.

Progress: This project is complete and has been published in Analytical Biochemistry. The article is attached.

Task 2. Identify integrin-associated signalling proteins in breast cells migrating on laminin-5, Months 6-30.

Progress: Much of the emphasis of this project has turned to examining the roles of specific signaling proteins (FAK, CAS, G proteins) and the work in progress is discussed above.

In addition, we have turned out attention to capitalizing on our finding that breast cells require Ca+2 to migrate, and this has spawned the development of a new project, described below:

Model for investigating integrin communication on laminin-1.

To metastasize, a breast tumor cell must adhere to, degrade, and migrate through the basement membrane. The family of extracellular matrix (ECM) molecules, the laminins, are rich in the breast basement membrane and can potentiate these processes to increase the metastatic potential of a tumorigenic breast cell. We therefore decided to build a model system for studying the interaction between laminins and the major cellular laminin ligand, the integrins.

Because it is the most thoroughly studied and well known laminin, we chose laminin-1 as a model integrin ligand. Laminin-1 exerts diverse biological activities such as stimulating cell adhesion, spreading, growth, and collagenase IV secretion. Ligand induced signal transduction by integrin/laminin-1 binding regulates intracellular pH, tyrosine phosphorylation, inositol lipid metabolism, and calcium (Ca2+) oscillations. The breast epithelial cell line MCF-10A interacts with laminin-1 using the integrins $\alpha1\beta1$, $\alpha3\beta1$, and $\alpha6\beta1$. Using function blocking anti-integrin antibodies, we found that blocking $\alpha1$, $\alpha6$ and $\beta1$ inhibit adhesion to laminin-1, whereas blocking $\alpha3$ stimulates adhesion of these cells (Figure 5). $\alpha3$ stimulation of adhesion is dominant over inhibition by blocking $\alpha1$. A second messenger stimulated by integrins that is required for breast cell adhesion is intracellular Ca^{2+}. Our results indicate that cells adhering to bound function blocking anti-integrin antibodies exhibit higher intracellular calcium flux on anti-$\alpha1$, and $\alpha6$ than on anti-$\alpha3$ and intact laminin-1 (Fig. 6). Furthermore, intracellular calcium flux is inversely proportional to strength of adhesion (Fig. 7). We conclude that MCF-10A response to laminin-1 is a function of the particular subsets of integrins engaged and that alterations in the type of integrin engaged will lead to altered calcium flux and cellular behavior.

In order to confirm these findings and to identify the mechanism of integrin cooperation in the regulation of integrin signaling cascades, we must be able to stimulate integrins independently and in concert. To accomplish this, we will identify fragments of laminin that each have only one integrin binding partner. Based on synthetic peptide studies, we conclude that there are eleven candidate domains of laminin-1. (Fig. 8) We have selected six domains that have a high probability of being a substrate for integrins $\alpha1$, $\alpha3$, and $\alpha6$. Because glycosylation and conformation are important for regulating integrin affinity, these fragments of laminin-1 are being produced in an insect cell expression system. After purification, each domain will be screened as a ligand for only one integrin. MCF-10A cells will be plated on individual domains that had only one integrin binding partner and on combinations of these domains. The contribution of each to cell adhesion and intracellular signaling cascades including calcium flux will be measured.

Task 3. Identify inhibitory compounds that block migration of malignant breast cells on laminin-5, Months 12-30.

a. Optimize assay. This is completed.

b. Screen inhibitors of biochemical signalling pathways in migration assays.

We have been unable to overcome our legal troubles with Polyfiltronics, and the 96 well plate we developed has not yet been produced. This in turn has hampered our ability to screen large numbers of unknown compounds collected by the Developmental Therapeutics Program at NIH. Instead, we turned our attention to a more modest survey, by examining the migration inhibiting properties of a small numebvr of derivatives of D-limonene. This project is described below:

We have developed an in vitro cell migration/cytotoxicity assay that, in conjunction with a proliferation assay, is able to discern the difference between cytotoxic and non-cytotoxic drugs that impede cell migration. Using non-cancerous, immortalized human breast cells, MCF-10A, as a control for normal tissue, we are able to screen compounds for possible harmful effects on normal tissue against those on cancerous tissue. In preliminary work on our migration assay, we decided to investigate perillyl alcohol, a plant-derived monoterpene, as a possible inhibitor of cancer cell migration.

Perillyl alcohol is currently in phase II clinical trials for its chemopreventive and chemotherapeutic effects to treat a variety of cancers including breast cancer. Distinct effects of perillyl alcohol on different types of cancer cell lines indicate that perillyl alcohol affects different oncogenic pathways in different types of cancer cell lines, or that perillyl alcohol affects a common oncongenic activity that may differ from cell line to cell line.

Our data indicate that non-cytotoxic doses of perillyl alcohol (Figure 9A,B) reduce cell migration in a dose-dependent manner in MCF-10A cells and MDA-MB 435 on fibronectin (Figure 10A,B) without significantly inhibiting adhesion of these cells to fibronectin (Figure 11A,B).

From these analyses, we conclude that perillyl alcohol is an attractive candidate for prophylactic treatment of breast cancer, because it inhibits cell movement at sub-lethal doses, and thus may contain the spread of pre-malignant cell populations.

Specific Aim 2: Identify the specific protein targets of compounds that inhibit migration of normal and malignant breast cells on laminin-5.

Progress: One area that we have progressed in is our analysis of the mechanism of action of perillyl alcohol. These results are described below:

One established monoterpene-induced biochemical modulation of interest is protein isoprenylation, which is important in maintaining the proper functioning of many proteins. Previous studies have demonstrated that perillyl alcohol is a competitive inhibitor of type 1 geranylgeranyl-protein transferase. Rac1 and RhoA of the Rho family of GTPases are both substrates for this enzyme and are important in the coordinated rearrangement of the actin cytoskeleton, which is required for cell migration.

The role of RhoA in stimulating the assembly of stress fibers and focal adhesions is better understood than how Rac1 or Cdc42 induces focal complex assembly. Activated RhoA binds to and activates the serine/threonine kinase Rho-kinase (Rock-2), which in turn phosphorylates and inhibits myosin light chain phosphatase. This inhibition results in increased phosphorylation of myosin light chain followed by enhanced myosin filament assembly and actin-activated myosin ATPase activity. Overall, through this pathway, RhoA activation results in bundling of actin filament into stress fibers and clustering of integrins into focal adhesions. This membrane-cytoskeleton interaction has been reported to increase invasiveness in tumor cells from liver and breast tissue. Additionally, the level of RhoA expression has been reported to be several times higher in tumors than in surrounding normal tissue. RhoA is also involved in a variety of other biological process such as cytokinesis, smooth muscle contraction, transformation and apoptosis.

GTPases have also been reported to play an important role in the metastatic behavior of tumor cells. Therefore, blocking the activation of these proteins by inhibiting their isoprenylation could reduce metastasis. Perillyl alcohol's mode of action in normal and malignant human breast cells is unknown. Thus, in determining the anticancer mechanism of perillyl alcohol, it is important to evaluate this biochemical effect in the particular cell type.

Using a phase separation assay, isoprenylated and unprocessed RhoA proteins were divided into detergent-enriched and aqueous phases of 1% Triton X-114 TBS buffer. After an 18-hour incubation, aqueous and detergent phases of MCF-10A cells were separated and subjected to Western blot analysis for RhoA. We observed a substantial increase in the percentage of RhoA in the aqueous phase of cells treated with 0.5 mM perillyl alcohol compared to control cells treated only with carrier (Figure 12).

Appendices

key research accomplishments

- Completion of the design and small scale manufacture of 96-well fluorescence-based cell migration plates
- Identification of RACK1 as an inhibitor of CHO cell migration.
- Identification of FAK as a laminin-5 signaling protein in human breast cells
- Identification of Ca+2 as an essential component of cell migration signaling in breast cells
- Identification of perillyl alcohol as a non-cytotoxic inhibitor of breast cell migration
- Determination that perillyl alcohol inhibits RhoA membrane association in breast cells

Reportable Outcomes:

manuscripts

Goldmann W, Alonso JL, Bojanowski K, Brangwynne C, Chen CS, Chicurel ME, Dike LE, Huang S, Lee KM, Maniotis A, Mannix R, McNamee H, Meyer CJ, Naruse K, Parker KK, Plopper G, Polte T, Wang N, Yan L and Ingber DE. Cell shape control and mechanical signaling through the cytoskeleton. In: Carraway K, ed. The Cytoskeleton and Signaling: A Practical Approach. Oxford, England: Oxford University Press, pp.245-276, 2000.

Rust, W.L., Huff, J.L., and Plopper, G.E. Screening assay for pro/anti-migratory compounds. Analytical Biochemistry 280:11-19, 2000.

Buensuceso, C.S., D. Woodside, J.L.Huff, G.E. Plopper, and T.E. O'Toole. The WD protein Rack1 mediates PKC and integrin dependent cell migration. Manuscript submitted, 2000.

abstracts

Rust, W.L., J.L. Huff, and G.E. Plopper. A high-throughput assay for screening anti-migratory compounds. Mol. Biol. Cell 10:267a, 1999.

Wagner, J.E., C. DiGennaro, J.A. Elegbede, W. Rust, and G.E. Plopper. Application of an automated, high-throughput assay to identify perillyl alcohol as a non-cytotoxic inhibitor of breast cancer migration. Mol. Biol. Cell 10:262a, 1999.

Carroll, K.J., V.J. Cavaretta, R.W. Bandle, J.L. Huff, M.A. Schwartz, V. Quaranta, and G.E. Plopper. Stimulation of breast cell migration on laminin-5 by antibody induced activation of $\alpha 3\beta 1$ integrin receptor and a $G\alpha i3$-mediated signaling pathway. Mol. Biol. Cell 10:339a, 1999.

Integrin signaling and cell migration on laminin-5, US Army Era of Hope Department of Defense Breast Cancer Research Program meeting June 8-11, 2000. Poster presentation by: George Plopper, Janice Huff, Will Rust, and Johanna Wagner.

presentations

None.

patents and licenses applied for and/or issued

Method for predicting the efficacy of anti-cancer drugs. W.L. Rust, J.L. Huff, and G.E. Plopper. Patent pending, 2000.

degrees obtained that are supported by this award

N/A

development of cell lines, tissue or serum repositories

N/A

informatics such as databases and animal models, etc.

N/A

funding applied for based on work supported by this award

1. National Institutes of Health, R21 Grant: Insight Awards to Stamp Out Breast Cancer. Title: In Vitro Screen for Inhibitors of Cancer Cell Migration. Total amount, $222,580. July 1, 2000- June 30, 2002. Submitted October 12, 1999.
2. Principle Investigator, US Army Breast Cancer Research Project Concept Proposal. Title: Structural derivatives of d-limonene as inhibitors of breast cell migration. Total amount, $75,000. Dates: July 1, 2000-Mune 30-2001. Submitted April 12, 2000.
3. Principle Investigator, UNLV Applied Research Program. Title: A UNLV/Biotechnology Collaboration. Total amount, $270,000. June 1, 2000-May 31, 2001. Submitted March 1, 2000.
4. Collaborator, 30% effort, National Institutes of Health Small Business Technology Transfer (STTR) Program, Phase I grant. Title: Migration/Death assay for tumor chemosensitivity testing (Janice Huff, PI). Total amount, $100,000. Dates: January 1, 2001-August 1, 2001. Submitted March 30, 2000.
5. Co-Principle Investigator, Fund for a Healthy Nevada Grant Program. Title: Early detection, treatment, and biology of lung cancer in Nevada women. Total amount, $1,608,099. Dates: December 1, 2000-November 30, 2002. Submitted August 22, 2000.
6. Co-Principle Investigator, National Institutes of Health AREA (R15) Award (Bingmei Fu, Principle Investigator). Title: Microvessel Permeability and Tumor Metastasis. Total amount, $135,500. August 1, 2000-July 31, 2002.

employment or research opportunities applied for and/or received based on experiences/training supported by this award

N/A

a copy of each of the above cited manuscripts and abstracts.

See attached.

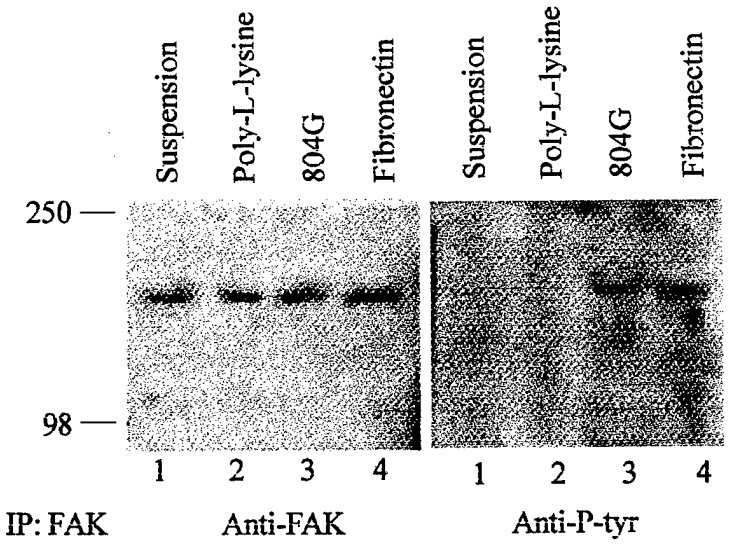

Figure 1. FAK is phosphorylated upon binding fibronectin and laminin-5. 4 million MCF-10A cells were trypsinized, held in suspension for 45 minutes, and plated on poly-L-lysine or fibronectin coated plates, or laminin-5 matrix deposited by 804G cells for 25 minutes. Adherent cells were lysed in RIPA. 500 μg of lysate was immunoprecipitated with anti-FAK monoclonal antibody and separated by SDS-PAGE. Western blot analysis with either anti-FAK or anti-phospho-tyrosine (P-tyr) mcAb.

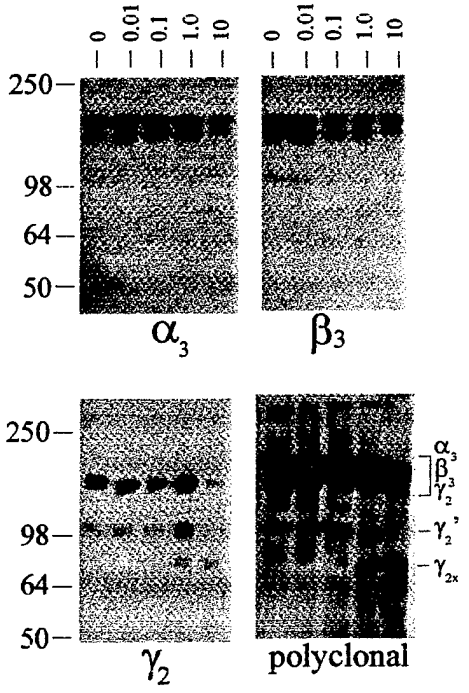

Figure 2. Laminin-5 matrix deposited by 804G cells were incubated at 37°with the indicated concentrations of elastase (μg/ml) for one hour. Matrix was then scraped in 8M urea sample buffer, and separated by SDS-PAGE. Western blots were conducted with the indicated anti-laminin antibodics.

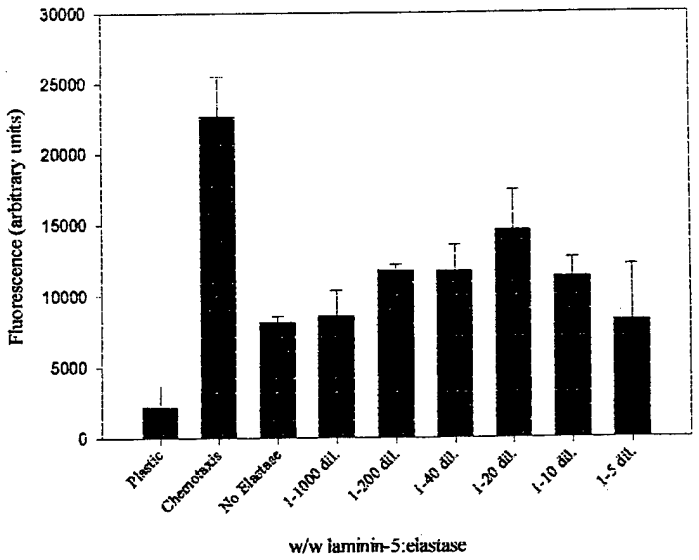

Figure 3. Pure laminin-5 was incubated at 37°C for one hour with the indicated w/w dilutions of elastase. The bottom of transwell migration filters were coated with 20μg/ml of the cleavage products. 120,000 MCF-10A cells were plated on the top of the filter in minimal media supplemented with 1mM sodium pyruvate and incubated for 18 hours. Non-migratory cells were wiped off, and the remaining cells were stained with the fluorescent dye calcein-AM (5uM). Migratory cells were quantified as the fluorescence intensity from the bottom of the filter. Error is represented as the standard deviation of 4 filters.

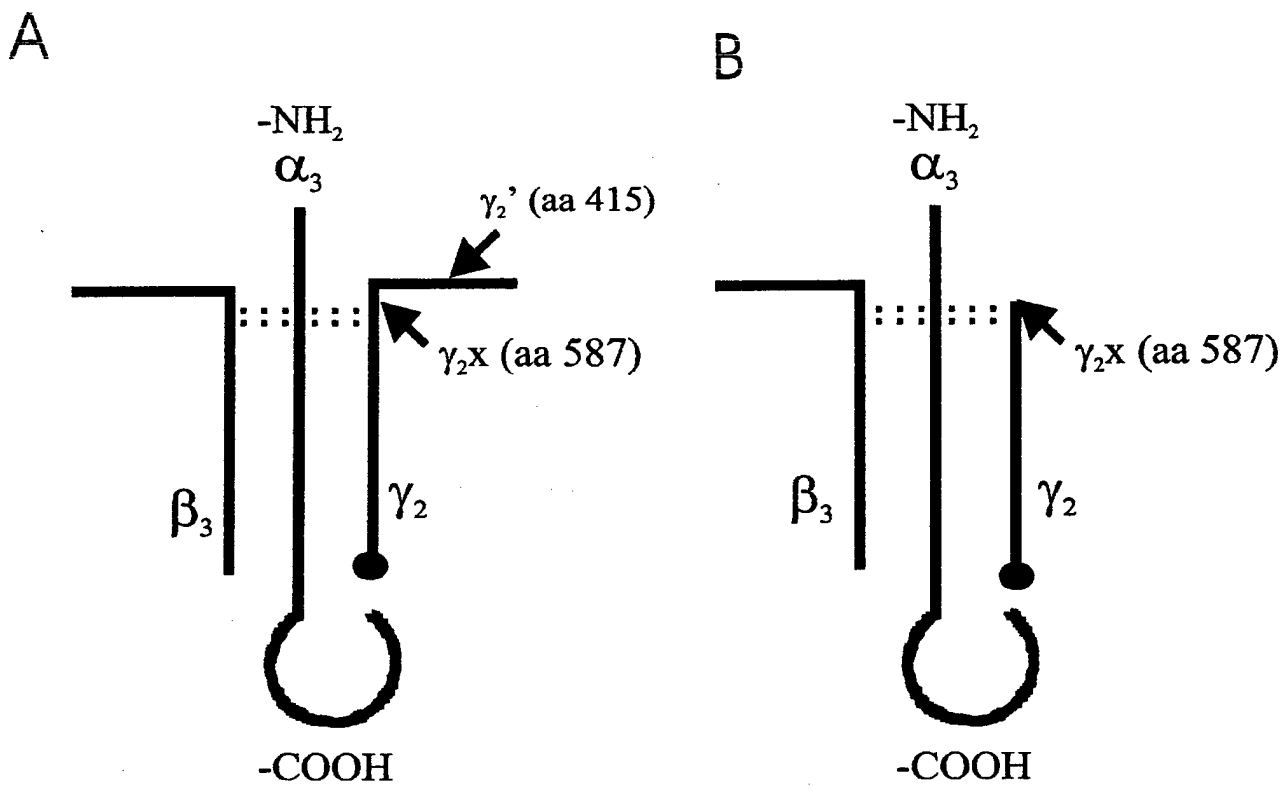

Figure 4. Diagram of Recombinant Laminin-5 γ2 Chain. A. Wild-type γ2 chain of the laminin-5 heterotrimer is cleaved by elastase upstream of two cysteine residues at the indicated positions. B. Laminin-5 containing a truncated γ2 chain, which has a deletion of all amino acid residues amino terminal to the elastase cleavage site. Both A and B are tagged at carboxyl terminus with a $(Histidine)_6$-tag.

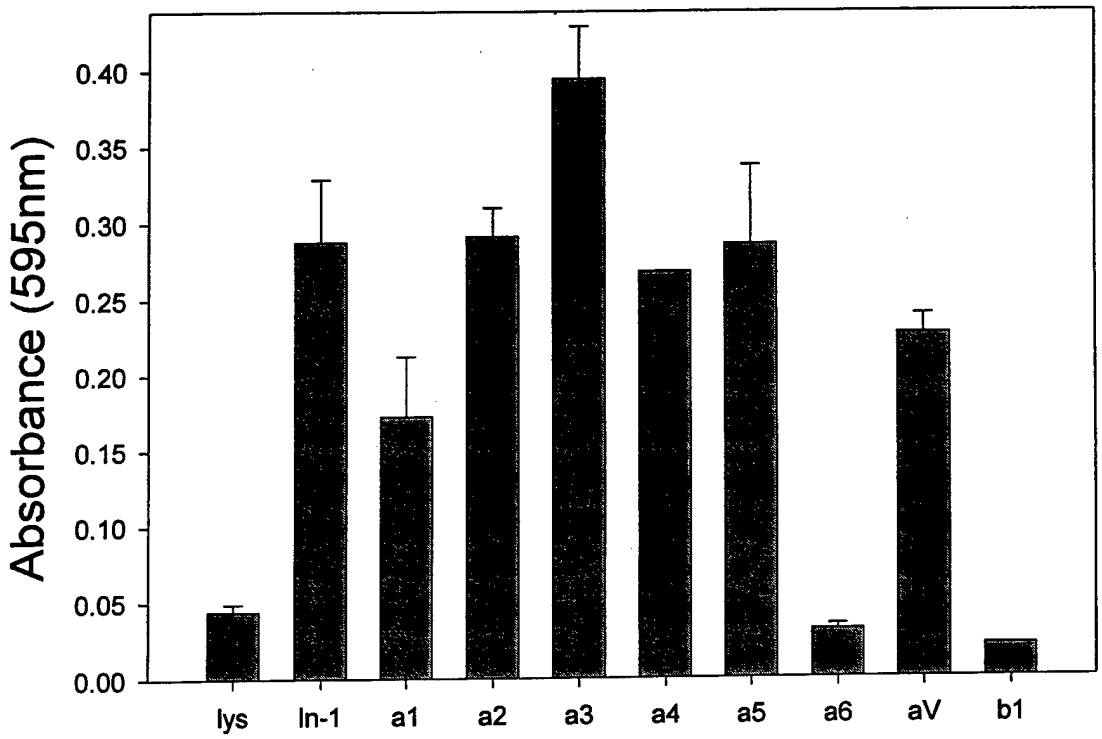

Fig. 5. MCF-10A adhesion to laminin-1 in the presence of anti-integrin function blocking antibodies. Cells were pre-incubated with antibodies for 30 mins. Prior to being added to wells coated with laminin-1. After 30 mins., adherent cells were stained with crystal violet, and absorbance measured.

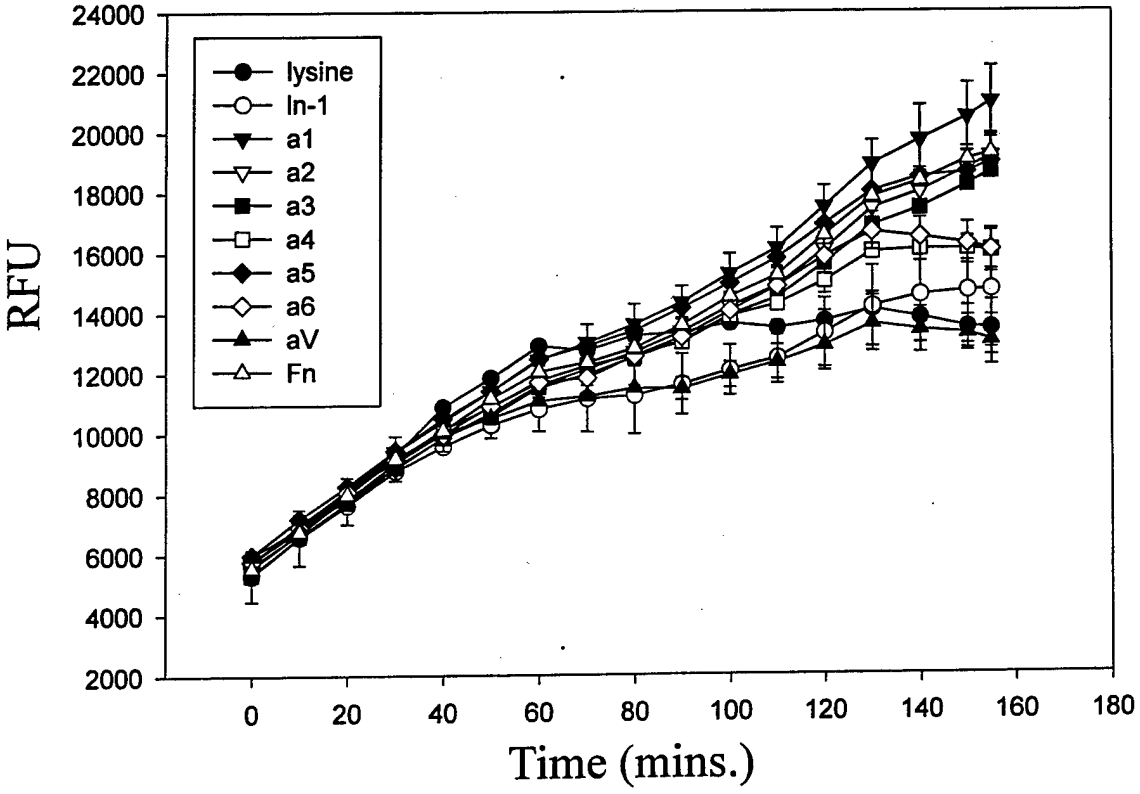

Fig.6 . Intracellular calcium release upon binding anti-integrin antibodies. MCF-10A cells were pre-incubated with the fluorescence calcium indicator Fluo-3 for 30 min and plated on bound anti-integrin antibodies at time zero.

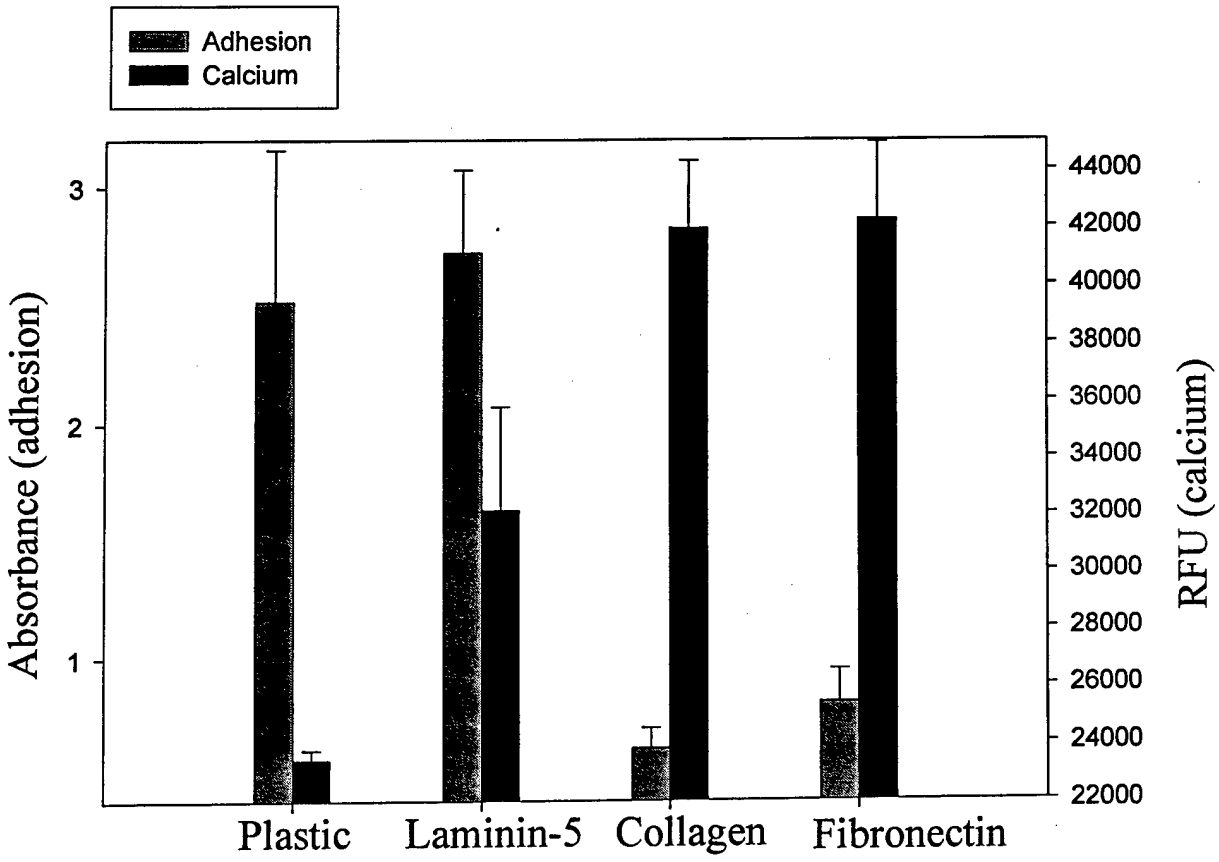

Fig. 7. Adhesion and calcium response to binding ECM. Adhesion and calcium measured as in previous figures.

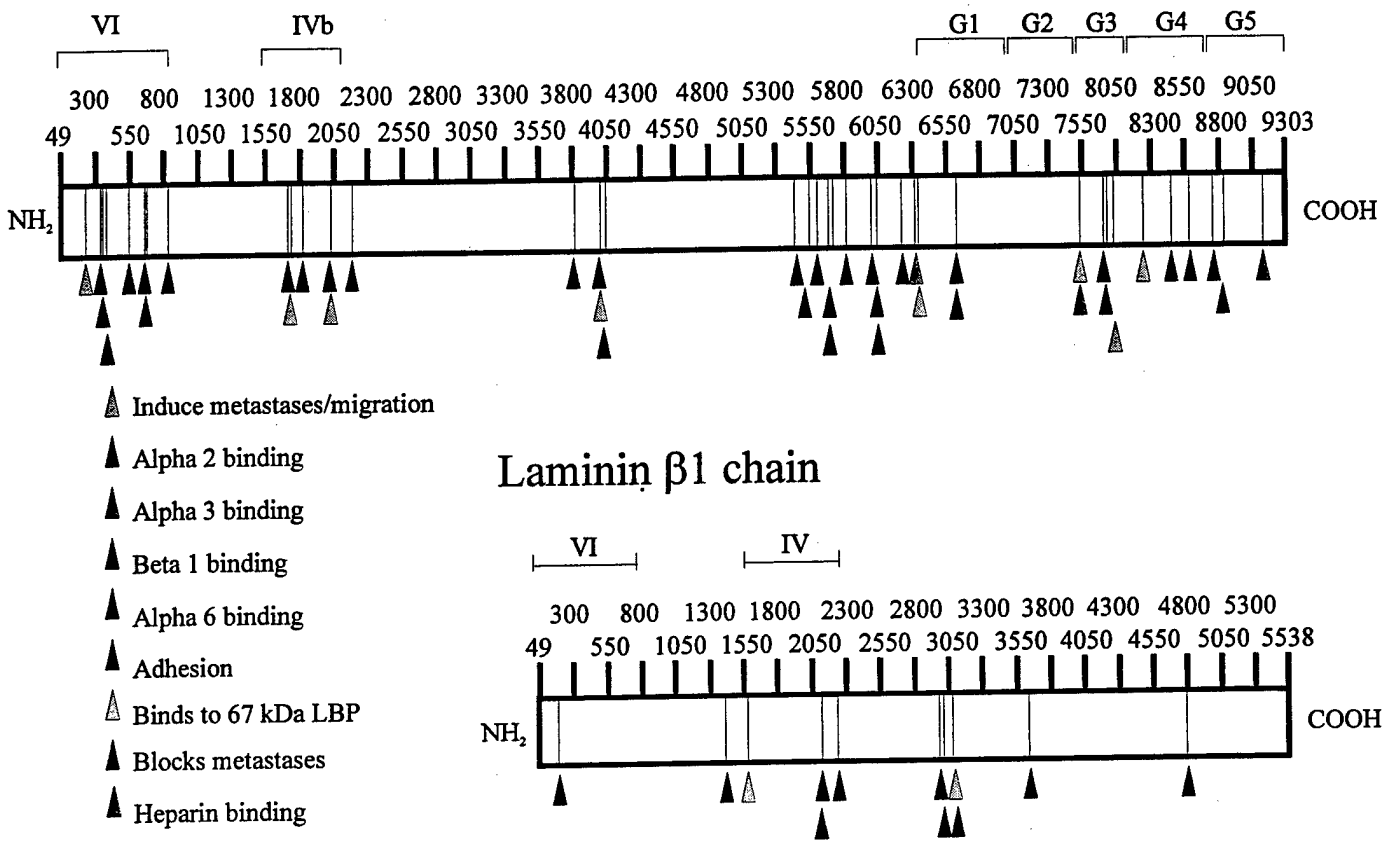

Fig.[8] . Functional analysis of laminin-1 chains by synthetic peptide screening. Domains are indicated above each chain.

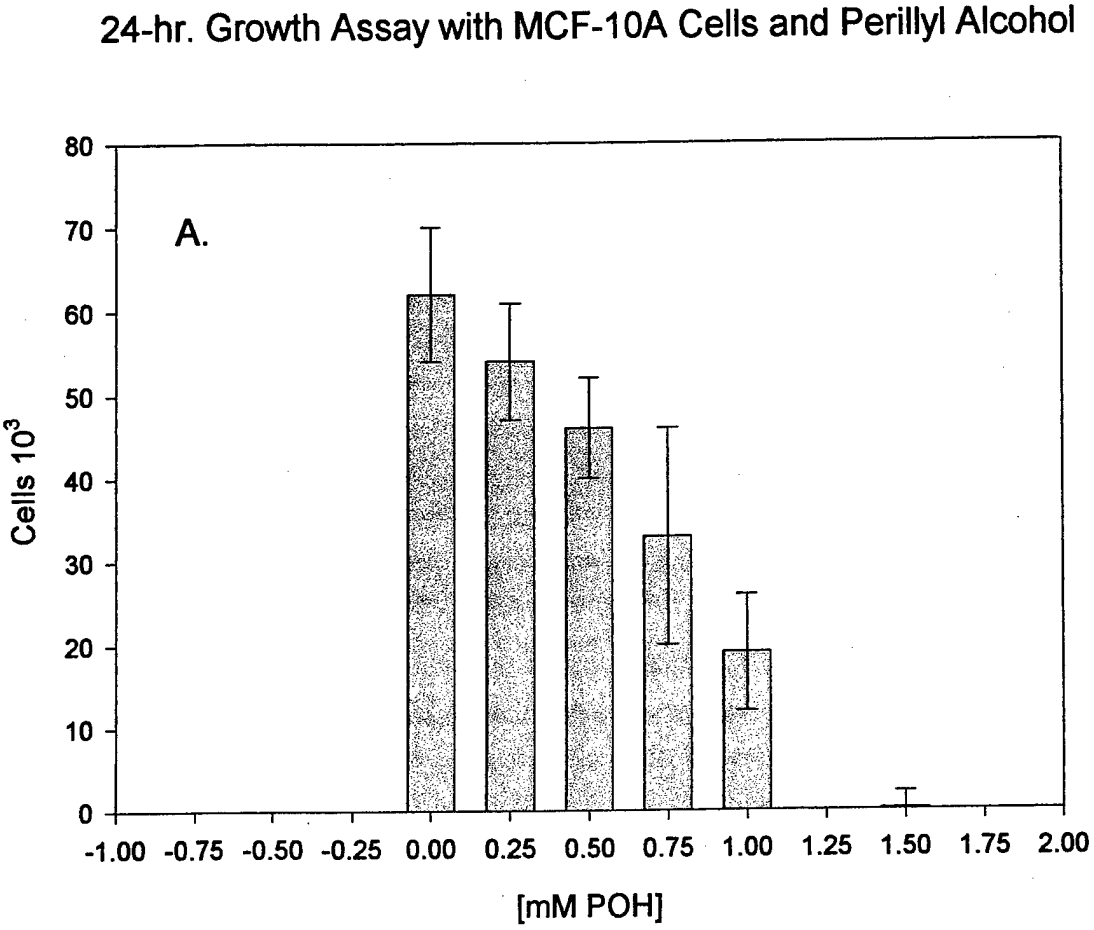

Figure9A The effect of perillyl alcohol (POH) on cell proliferation was measured by a 24-hour growth assay. $3x10^3$ cells were plated in replicates of 12 in 96-well plates in the presence of increasing concentrations of POH. After 24 hours, cells were fixed and stained. Growth was quanitated by measuring absorbance with the Tecan Spectra Fluor, a computer-controlled fluorometer. A. MCF-10A cells; immortalized, non-tumorigenic human breast cells B. MDA-MB cells; metastatic human breast cells.

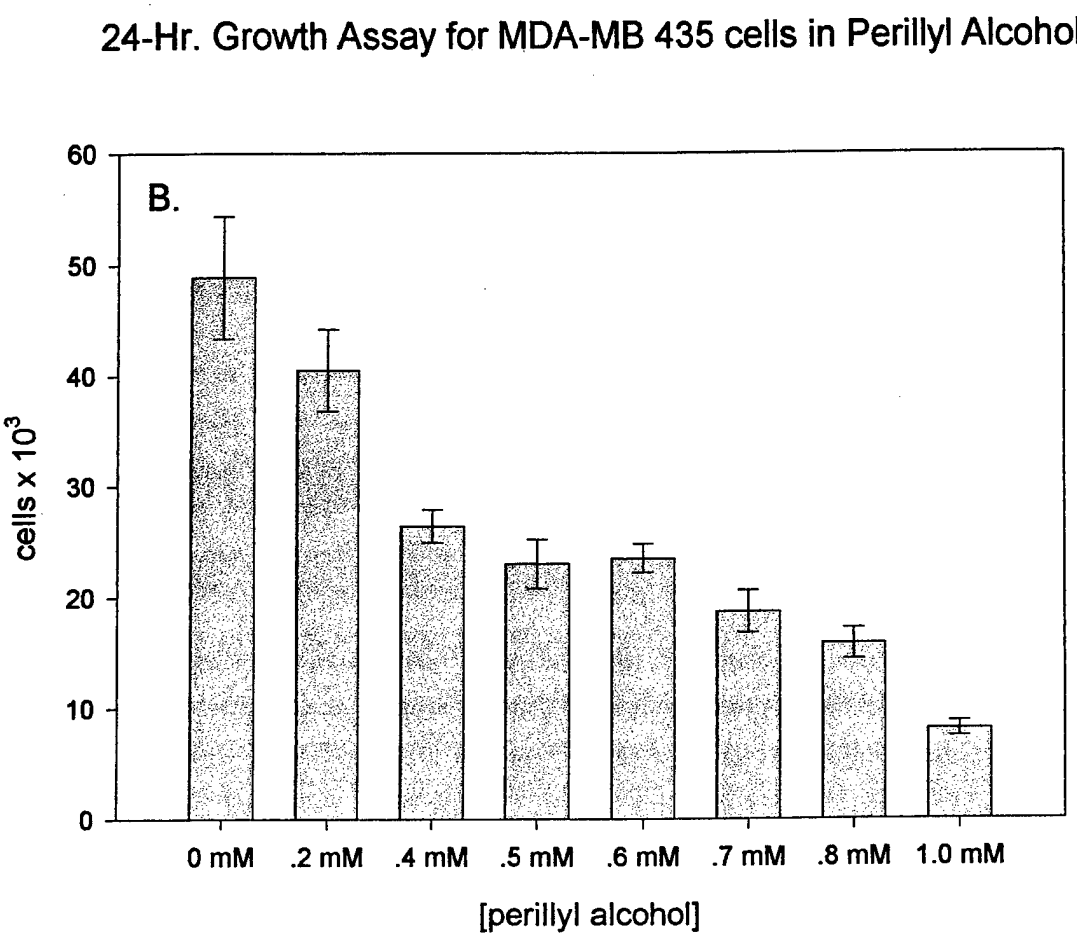
24-Hr. Growth Assay for MDA-MB 435 cells in Perillyl Alcohol
B.
cells x 10^3
60
50
40
30
20
10
0
0 mM
.2 mM
.4 mM
.5 mM
.6 mM
.7 mM
.8 mM
1.0 mM
[perillyl alcohol]

Figure 9 B.

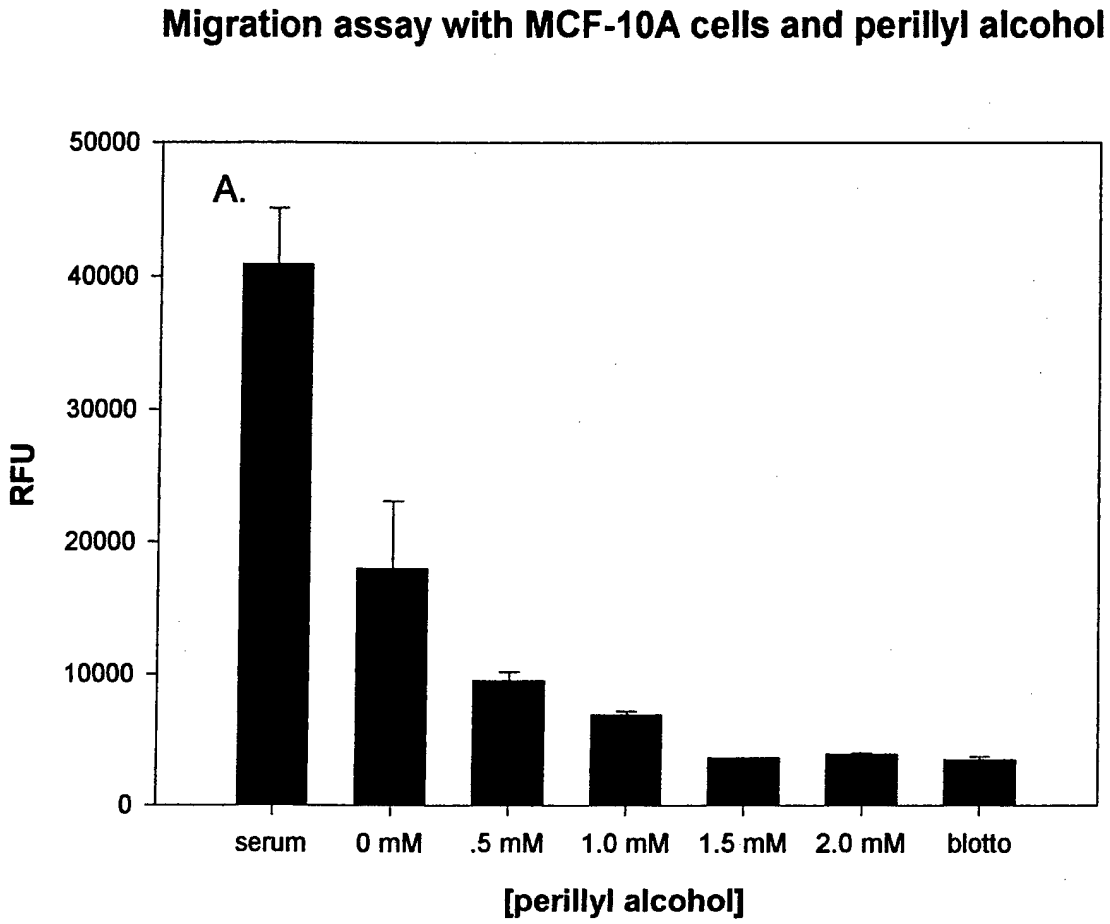

Figure 10. The effect of perillyl alcohol (POH) on haptotactic migration. Prior to plating cells were preincubated in the test concentrations of POH for 30 min. at 37C. $12x10^4$ cells were plated in replicates of 4 on transwell migration plates. Filters wer coated with fibronectin and cells were allowed to migrate for 18 hours at 37C. During the last 30 min. of the assay, the fluorescent, live cell indicator, calcein-AM was added. Migration was measured in a plate reader. A. MCF-10A cells B. MDA-MB 435

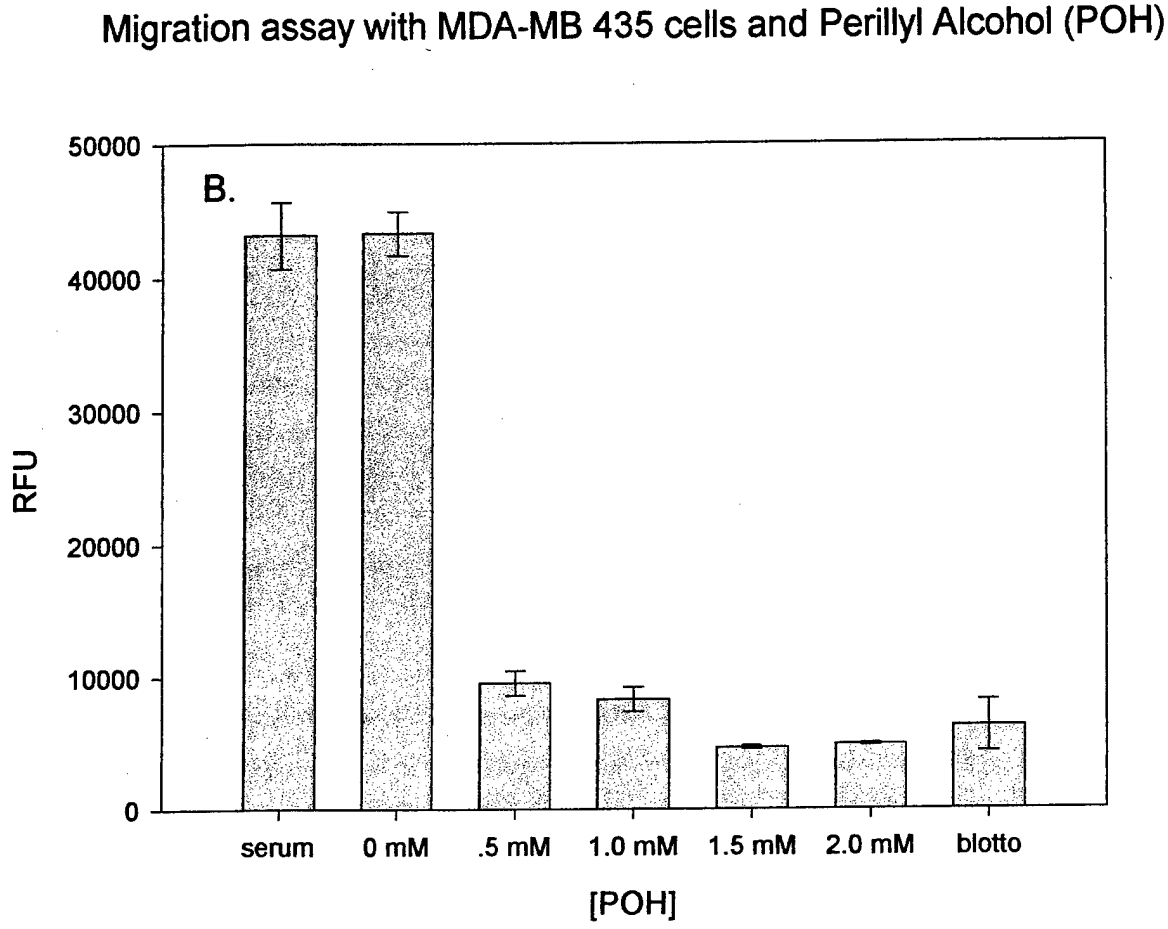
Migration assay with MDA-MB 435 cells and Perillyl Alcohol (POH)
B.
RFU
50000
40000
30000
20000
10000
0
serum
0 mM
.5 mM
1.0 mM
1.5 mM
2.0 mM
blotto
[POH]

Figure 10B.

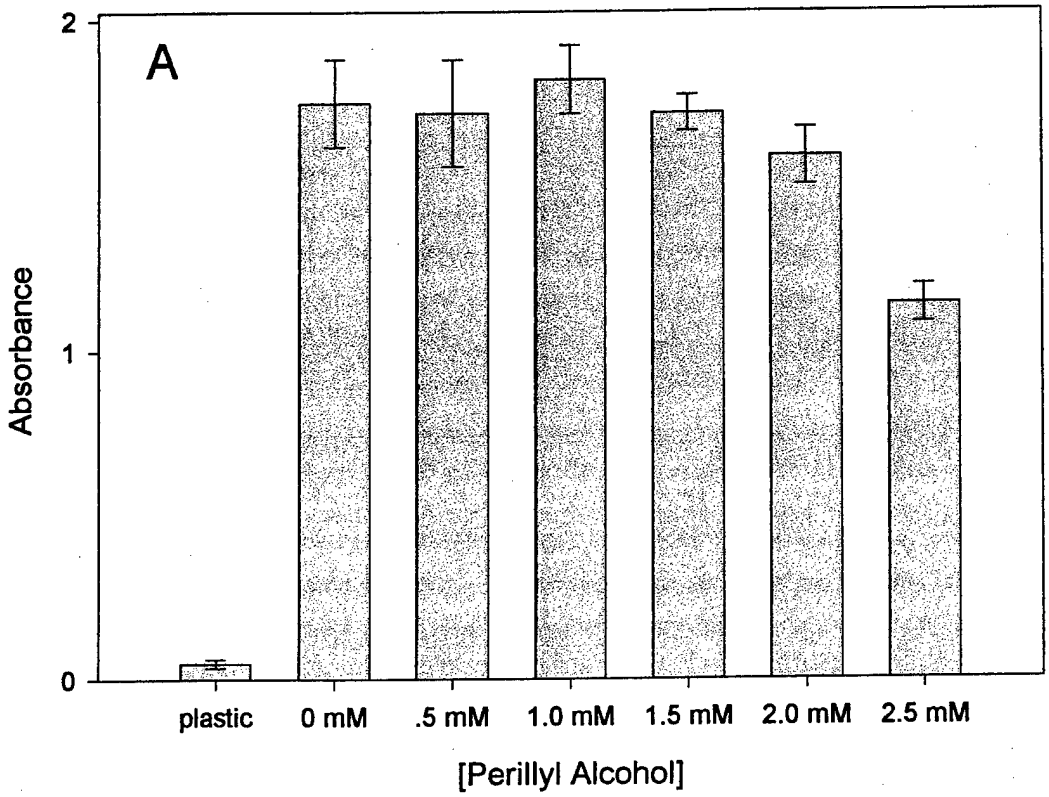

Figure 11 The effect of perillyl alcohol (POH) on cell adhesion. $12x10^4$ cells were plated in replicates of 8 in 96-well plates coated with fibronectin in the presence of increasing concentration of POH. A. MCF-10A cells B. MDA-MB 435 cells

Adhesion assay with MDA-MB 435 cells and Perillyl Alcohol on FN

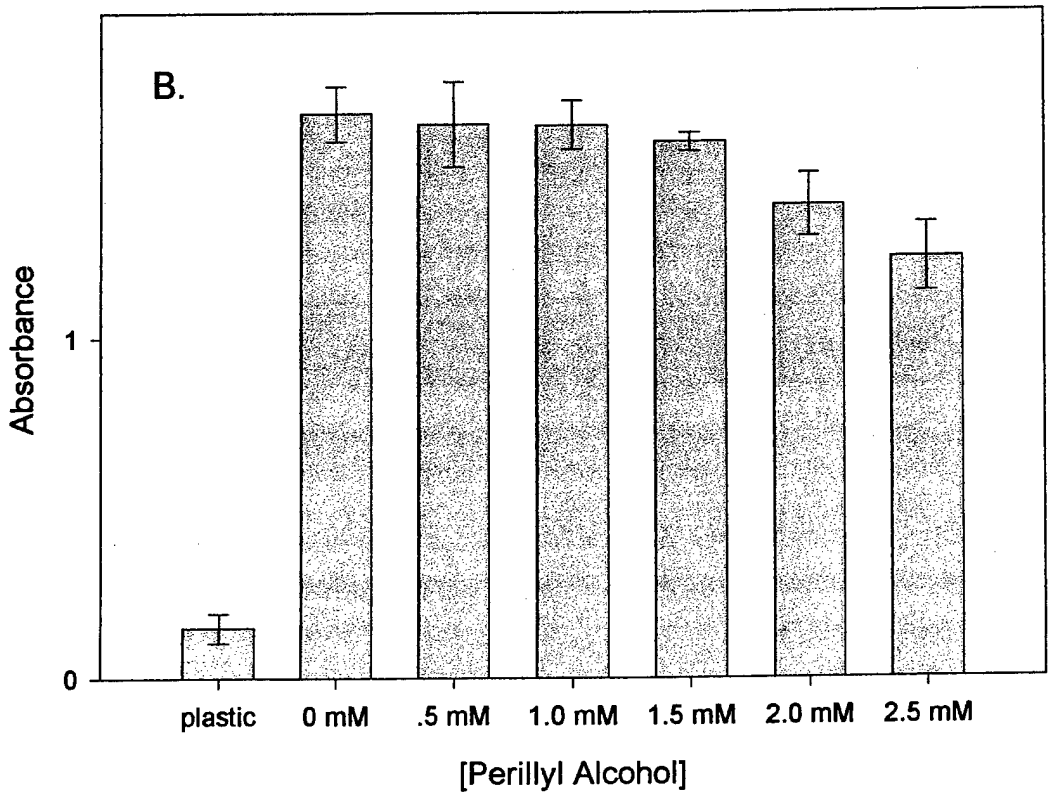

Figure 11B.

Immunoprecipitation and SDS-PAGE for RhoA protein (26 kD)

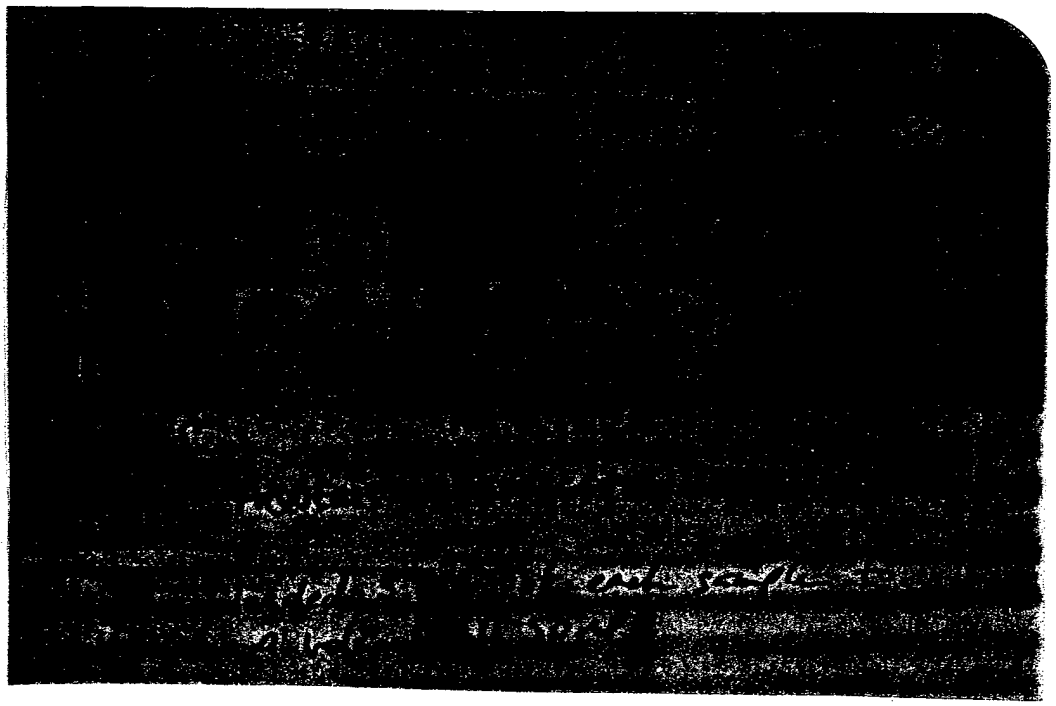

Figure 12 Phase separation assay using Triton X-114. After 18 hours of exposure to AM media, 0 mM or .5 mM perillyl alcohol in MEM media MCF-10A cells were lysed directly in 1% Triton X-114 in TBS buffer. After 10 min on ice with occasional mixing, insoluble material was removed by centrifugation at 10,000 g for 10 min at 4C. The supernatants were transferred into new tubes and warmed at 37C in a water bath for 2 min. The turbid solution was centrifuged at 10,000 g for 2 min at room temperature. The upper phase was the aqueous phase (detergent-depleted) and the lower phase was the detergent –enriched phase. After this 3.7% of each sample was brought up to a volume of 50 microliters with TBS followed by immunoprecipitation and SDS-PAGE.

Analytical Biochemistry **280,** 11–19 (2000)
doi:10.1006/abio.2000.4510, available online at http://www.idealibrary.com on IDEAL®

Screening Assay for Promigratory/Antimigratory Compounds

Will L. Rust, Janice L. Huff, and George E. Plopper[1]
Department of Biological Sciences, University of Nevada, Las Vegas, 4505 Maryland Parkway, Box 454004, Las Vegas, Nevada 89154

Received November 8, 1999

Large-scale screening strategies aimed at finding anticancer drugs traditionally focus on identifying cytotoxic compounds that attack actively dividing cells. Because progression to malignancy involves acquisition of an aggressively invasive phenotype in addition to hyperproliferation, simple and effective screening strategies for finding compounds that target the invasive aspects of cancer progression may prove valuable for identifying alternative and preventative cancer therapies. Here, we describe a fluorescence-based automated assay for identifying antimigratory compounds, with the ability to discern cytotoxic from noncytotoxic modes of action. With this assay, we analyzed the effects of two drugs on tumorigenic (MDA-MB-435) and nontumorigenic (MCF-10A) human breast cell lines. We chose to compare carboxyamidotriazole (CAI), an experimental compound shown to inhibit migration of various cell types, with tamoxifen, a common preventative and therapeutic anticancer compound. Our assay demonstrated that both these compounds inhibit migration at sublethal concentrations. Furthermore, CAI was more effective than tamoxifen at inhibiting chemotactic and haptotactic migration of both cell lines at all concentrations tested.

Key Words: **migration; cytotoxicity; screening; CAI; tamoxifen.**

Cancer progresses in two general stages. It begins as a carcinoma of clonal, hyperproliferating cells confined to the tissue of origin, which may exist for years as a benign, primary tumor. The conversion of a benign tumor to malignancy involves the acquisition of an aggressively invasive phenotype, wherein the cancer cells leave the tissue of origin and establish new tumor metastases at distant sites. Metastases are first evident at local lymph nodes, with the severest patient prognosis associated with metastases located at distant sites (1).

There are limitations to common chemotherapy regimens. The most common drugs for treating solid-tissue cancers are cytotoxic compounds that interfere with the synthesis or function of nucleic acids. These drugs target actively dividing cells of established tumorigenic colonies (2). While many are effective at treating earlier stage cancers, none are curative for later stage disease, when overt metastases are already evident. Because many tumors are not diagnosed until advanced stages, the effectiveness of these drugs is limited (3). In addition, these antiproliferative agents produce damage to normal tissues, such as immune suppression, mucositis, and hair loss, as well as side effects such as nausea and vomiting (2, 4). It is important, therefore, to identify alternative, and potentially less toxic, treatments for halting the spread of cancer. These strategies focus on preventing the conversion of tumorigenic cells to the malignant phenotype, as opposed to arresting cell growth. For example, recent chemotherapeutic advancements include the introduction of compounds with noncytotoxic mechanisms of action, such as antiangiogenic factors, growth factor antagonists, interferons, and agents that induce cellular differentiation (5–8). These noncytotoxic compounds will potentially be used to prevent the spread of cancer as well as to increase the effectiveness of cytotoxic drugs. Since the conversion from hyperproliferative to invasive disease typically takes many years, a large window exists for the use of preventative therapies (1, 3).

The cellular changes required for malignant conversion are complex, offering a large and diverse array of potential targets for the development of antimetastatic drugs. A common theme among these cellular changes is aberrant regulation of cell migration. Examples of these changes include secretion of proteases, decreased synthesis of protease inhibitors, loss of cell–cell con-

[1] To whom correspondence should be addressed. Fax: (702) 895-3956. E-mail: plopper@nye.nscee.edu.

0003-2697/00 $35.00

tacts, modifications of cell–substrate interactions, and alteration in the response to and production of chemotactic and haptotactic stimuli during tumor-induced angiogenesis and/or metastasis (reviewed in 9–11). The identification of compounds that halt cell migration without inducing cell death may lead to creation of novel compounds that are less toxic than common antiproliferative agents (3).

Carboxyamido-triazole (CAI)[2] is an example of such an antimigratory compound, which is currently in stage 2 clinical trials of androgen-independent prostate cancer (12). CAI is an inhibitor of non-voltage-gated calcium channels and blocks cell migration or invasion in breast cancer cell lines (13), prostate cancer cell lines (14), ovarian cancer cell lines (3), and head and neck squamous cell carcinomas (15). The antiproliferative effect of CAI is cytostatic, not cytotoxic, as cells will recover after the removal of CAI (14, 16). This indicates that CAI inhibits signal cascades specific to migration and proliferation. Established modes of action for CAI include inhibition of nucleotide metabolism by depleting phosphoribosyl pyrophosphate (16), inhibition of arachidonic acid and phophoinositide generation (17), and reduction of matrix metalloproteinase activity (13, 18).

While compounds such as CAI hold promise for effective cancer therapy, there is a lack of screening strategies aimed at identifying these noncytotoxic, antimigratory compounds. Here we present a fluorescence-based, high-throughput method for screening potential antimigratory compounds that is designed to discern cytotoxic from noncytotoxic mechanisms of action. Using 96- and 24-well migration filter plates with fluorescence-opaque filters, we show that cell migration can be quantitated easily and reliably with the use of the fluorescent dye calcein-AM. Cytotoxicity of compounds tested is determined by labeling nonmigrated cells with the fluorescent DNA intercalator propidium iodide. The experimental cells are doubly labeled so that migration and cytotoxicity are measured in the same assay. The use of a high-throughput format, and the novel incorporation of screens for both antimigration and cytotoxicity on the same test cells, represent major improvements in efficiency and cost over traditional transfilter migration assays.

With this method, we analyzed the effects of CAI and the well-established anti-breast cancer compound tamoxifen on migration and viability of two human breast cell lines. Both compounds inhibited migration of the breast cancer cell line MDA-MB-435 and the nontumorigenic breast cell line MCF-10A at subcytotoxic concentrations. Our assay demonstrated that, while MDA-MB-435 cells showed resistance to CAI-induced cell death, CAI inhibited haptotactic and chemotactic migration of both cell lines more effectively than tamoxifen.

[2] Abbreviations used: CAI, carboxyamido-triazole; PBS, phosphate-buffered saline; RFU, relative fluorescence units; MTT, 3-[4,5-dimethylthiazol-2-yl]-2,5-diphenyltetrazolium bromide; ER, estrogen receptor.

MATERIALS AND METHODS

Materials

MTT (3-[4,5-dimethylthiazol-2-yl]-2,5-diphenyltetrazolium bromide; Thiazolyl blue) was purchased from Sigma–Aldrich Chemicals (St. Louis, MO). Calcein-AM was purchased from Molecular Probes (Eugene, OR). Tamoxifen citrate was purchased from Calbiochem–Novabiochem (La Jolla, CA). Carboxyamido-triazole (CAI) was a generous gift of Dr. Elise C. Kohn (Laboratory of Pathology, National Cancer Institute, National Institutes of Health, Bethesda, MD). Ninety-six-well fluorescence-blocking migration plates were provided by Polyfiltronics (Rockland, MA). Twenty-four-well fluorescence-blocking migration plates were a generous gift of Dr. Nancy Chung-Welch (Becton Dickinson, Bedford, MA). Information regarding the commercial availability of the 24- and 96-well fluorescence-blocking migration plates can be found at the Becton Dickinson Web site (www.bd.com/labware/newprod/fluoroblok.html). Transwell migration plates were purchased from Costar (Cambridge, MA).

Tissue Culture

MCF-10A and MDA-MB-435 cells were maintained as previously described (19). Cells were routinely passaged using trypsin/EDTA (Irvine Scientific).

Transwell Migration Assay

Migration assays were conducted as previously described (20), with the following modifications. Transwell filters (8.0-μm pore size, Costar) were coated with purified bovine fibronectin, mouse laminin-1, and collagen IV at 20 μg/ml in carbonate buffer (pH 9.3) for 1 h at room temperature. A sample consisting of 120,000 cells was suspended in DME with 292 μg/ml L-glutamine, 100 U/ml penicillin g, 100 μg/ml streptomycin sulfate (GPS, Irvine Scientific, Santa Ana, CA), and 1 mM sodium pyruvate (GIBCO BRL, Grand Island, NY), plated on the uncoated side of the filter, and incubated in a humidified incubator containing 5% CO_2. Filters were washed twice in phosphate-buffered saline (PBS), and the uncoated side of each filter was wiped with a cotton-tipped applicator to remove cells that had not migrated. Cells were then fixed in 3.7% formaldehyde for 15 min and stained with crystal violet as in the adhesion assay. Stained cells of four representative fields of each filter were counted at 400× magnification.

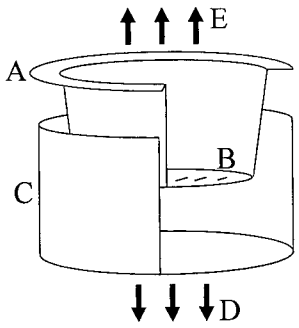

FIG. 1. Individual filter insert and feeder well of a 24- or 96-well migration plate. Test cells are loaded into filter insert A and allowed to migrate across a fluorescence-opaque filter B toward media in feeder well C. Cells are subsequently labeled with fluorescent indicators of cell migration and cell death. Emitted fluorescence of migrated cells is measured from underneath the filter D. Emitted fluorescence of nonviable cells is measured from above the filter E.

96- and 24-Well Fluorescence Migration Assay

An individual filter insert and well of a 24- or 96-well migration plate is indicated in Fig. 1. Both 24-well and 96-well migration plates are designed as a single insert containing all filter wells in one piece. Each filter insert (A) has a UV-opaque membrane (B) with 8.0-μm pores. Inserts fit into a well (C) of a 24- or 96-well reservoir plate. The undersides of the filters were left uncoated or were coated with 20 μg/ml bovine plasma fibronectin, type IV collagen, or laminin-1 (GIBCO BRL) in 0.1 M acetic acid and allowed to evaporate. The filter insert was submersed in wells of feeder plate containing DME with 1× GPS and 1 mM sodium pyruvate or DME supplemented with 1× GPS and 10% FCS. A sample of 100,000 cells suspended in DME with 1× GPS and 1 mM sodium pyruvate was added to the inside of each filter well (80 and 100 μl for the 96- and 24-well plates, respectively). For drug studies, drugs were added to the cell suspension immediately before loading cells onto the migration plate. Thirty minutes before the end of the migration assay, calcein-AM was added to the feeder wells at a final concentration of 5 μM. Filters and wells were washed twice in PBS to remove excess dye. Fluorescence of calcein-AM-labeled cells was measured from the bottom of the plate (D) in a Tecan SpectraFluor plate reader (Research Triangle Park, NC), with 485-nm excitation and 530-nm emission filters. As an indicator of cell death, propidium iodide fluorescence was measured from the top of the filter insert (E).

Quantification of Cell Death

Cells grown in 96-well plates were incubated for 4 h in 200 μl per well of the appropriate media supplemented with 1.25 mg/ml MTT (3-[4,5-dimethylthiazol-2-yl]-2,5-diphenyltetrazolium bromide; Thiazolyl blue). To release reduced MTT from viable cells, 150 μl of media was replaced with acidic 2-propanol (99.7% 2-propanol, 0.3% 12.1 N HCl) and wells were incubated overnight at room temperature. Absorbance was measured at 570 nm vs 630 nm reference using a Tecan SpectraFluor. Quantification of cell death by fluorescence was performed as previously described (21). Briefly, 1.2 mM propidium iodide was added to media of test wells or filters to reach a final concentration of 30 μM and incubated for 30 min at 37°C. As a positive control, cells were lysed in 1% Triton X-100 (Sigma) detergent during incubation with propidium iodide. Fluorescence of incorporated dye was measured at 560-nm excitation and 645-nm emission wavelengths using a Tecan SpectraFluor.

Statistical Analysis

ANOVA/*t* test was performed on data from indicated figures using a 95% confidence interval. All experiments were conducted at least three times with four to sixteen replicates per condition.

RESULTS

Fluorescence of Labeled Cells Correlates Linearly with Cell Number

In order to quantify migrated cells automatically, cells were labeled with the live cell fluorescent indicator calcein-AM, and a standard curve comparing relative fluorescence units (RFU) vs cell number was obtained (Fig. 2). Specific numbers of prelabeled MCF-10A cells were plated in a 96-well tissue culture plate and RFU measurements of these cells correlated linearly with cell number (Fig. 2A). Because the plate reader parameters and dimensions of the plates are slightly different in a migration assay, we confirmed this correlation of cell number with RFU on migratory cells on the bottom of the migration filter. MCF-10A cells were allowed to migrate toward serum through transparent transwell filters. Nonmigratory cells were removed from the upper wells, and migratory cells measured by both calcein-AM labeling and visual counting of cells in five representative fields of each filter (Fig. 2B). Similar results were observed with MDA-MB-435 cells (data not shown).

A UV-Opaque Membrane Allows for Detection of Migratory vs Nonmigratory Cells

The use of a fluorescence-opaque membrane simplifies migration assays and allows separate detection of fluorescently labeled cells on either side of the membrane. The absorption spectrum of the membrane used in our assay is effective at blocking a UV signal through the membrane if either the emission or excitation wavelength of the fluorescent indicator used

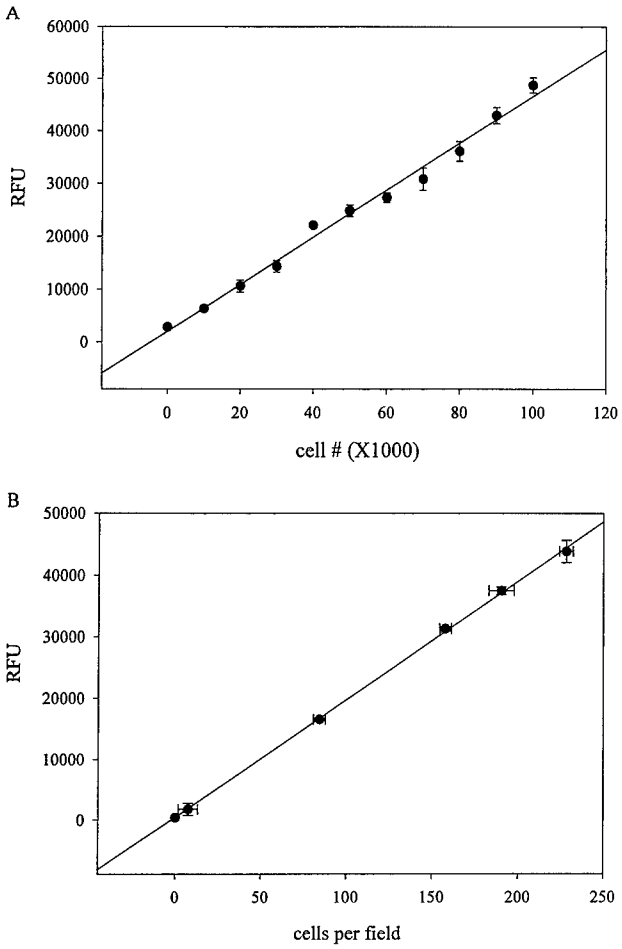

FIG. 2. Calcein-AM fluorescence correlates linearly with cell number. (A) The indicated number of prelabeled MCF-10A cells was plated in a 96-well plate and fluorescence intensity measured. (B) Chemotactic migration of 30,000–120,000 MCF-10A cells was measured in a transwell migration filter by calcein-AM fluorescence (y axis), and subsequently the cells were fixed and stained, and representative fields counted (x axis). Error is represented as the standard deviation of 8 wells.

falls within the absorption band (data not shown and Ref. 22). These filters effectively block the fluorescence (>95%) from the opposite side of the membrane of either of the dyes used in our assays (data not shown and Ref. 22). This membrane simplifies endpoint analysis by eliminating the need to remove nonmigratory cells before quantifying migratory cells. MCF-10A and MDA-MB-435 cells were allowed to migrate through fluorescence-opaque filters of 96- or 24-well filter plates toward serum (chemotaxis) or the indicated matrices (haptotaxis), and migration was quantified by calcein-AM labeling (Fig. 3). The data in Fig. 3 demonstrate that both cell lines migrated more toward fibronectin than other matrices. For this reason, fibronectin was chosen as the haptotactic stimulus for all drug studies. Note that fluorescence values for each cell line cannot be directly compared to each other as different cell lines exhibit different labeling efficiencies. For example, MCF-10A cells emit a fluorescence that can be as much as 40% brighter than that emitted by similarly labeled MDA-MB-435 cells (data not shown).

Cytotoxic Properties of Drugs Can Be Discerned from Antimigratory Properties with the Fluorescent Indicator Propidium Iodide

Because a cytotoxic compound will halt migration by killing cells, the cytotoxic effects of tested compounds must be evaluated in screens for antimigratory drugs. To this end, we incorporated a fluorescence-based cytotoxicity assay that was performed in the upper well of the migration plate immediately following the migration assay. This protocol was adapted from Nieminen *et al.* (21). The DNA intercalator propidium iodide is a cell-impermeant dye whose fluorescence is increased 10-fold upon binding DNA (23). The dye is incorporated into membrane-compromised, nonviable cells and is excluded from viable cells. Propidium iodide was added to the upper well of the migration plate 30 min before the end of the migration assay. Propidium iodide fluorescence measurements inversely correlated with results obtained with the 3-[4,5-dimethylthiazol-2-yl]-2,5-diphenyltetrazolium bromide (Thiazolyl blue; MTT) cell viability assay in experiments where cells were exposed to increasing concentrations of sodium azide (Fig. 4). Similar results were seen when cells were exposed to tamoxifen and sodium arsenite (data not shown). Therefore, propidium iodide uptake can be used as a quick and reliable indicator of cell death.

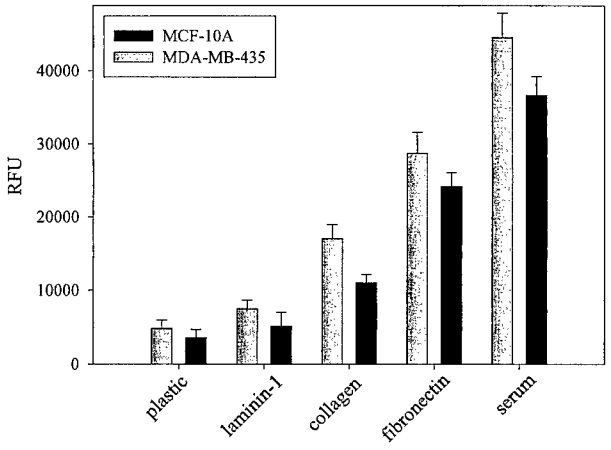

FIG. 3. MCF-10A and MDA-MB-435 cells each migrate with different strength toward serum and bound matrices. A sample of 120,000 cells was allowed to migrate toward the indicated stimulus in 24- and 96-well filter plates with fluorescence-opaque filters. Migrated cells were quantified by calcein-AM fluorescence. Error is represented as the standard deviation of 16 wells.

The Potential Antimetastasis Drug CAI and the Common Anti-Breast Cancer Drug Tamoxifen Inhibited Breast Cell Migration at Noncytotoxic Concentrations

To demonstrate the effectiveness of our assay for measuring antimigratory and cytotoxic properties of drugs, we compared CAI and tamoxifen on a nontumorigenic and a highly metastatic breast cancer cell line. Both tamoxifen and CAI inhibited migration in a dose-dependent manner at sublethal concentrations, and CAI was more effective than tamoxifen at halting migration in all cases (Fig. 5). Haptotactic migration on fibronectin was more sensitive to drug effects than chemotactic migration toward serum of both cell lines (Figs. 5A–5D). MCF-10A cells exposed to 10 μM CAI demonstrated a 45% inhibition of haptotactic migration (Fig. 5C). At 20 μM CAI, haptotaxis of these cells was completely abolished, and chemotaxis was inhibited 33%. In contrast, 10 μM tamoxifen inhibited MCF-10A haptotaxis by only 17%. At 20 μM, tamoxifen abolished haptotactic migration of MCF-10A cells and inhibited chemotaxis by 27% (Fig. 5A). MDA-MB-435 cells exposed to 10 μM CAI demonstrated 32% inhibition of chemotaxis and 7% inhibition of chemotaxis. At 20 μM, CAI abolished haptotaxis and inhibited chemotaxis by 42% (Fig. 5D). MDA-MB-435 cells exposed to tamoxifen, however, demonstrated nonsignificant inhibition of chemotaxis and haptotaxis at 10 μM, and, at 20 μM, only 51% inhibition of haptotaxis and 9% inhibition of chemotaxis (Fig. 5B). In addition, MCF-10A cell viability was more sensitive to CAI than MDA-MB-435 cells, as evidenced by increased propidium iodide fluorescence (Figs. 5C and 5D). Vehicle alone (DMSO, 95% ethanol) did not significantly affect migration in any case (data not shown).

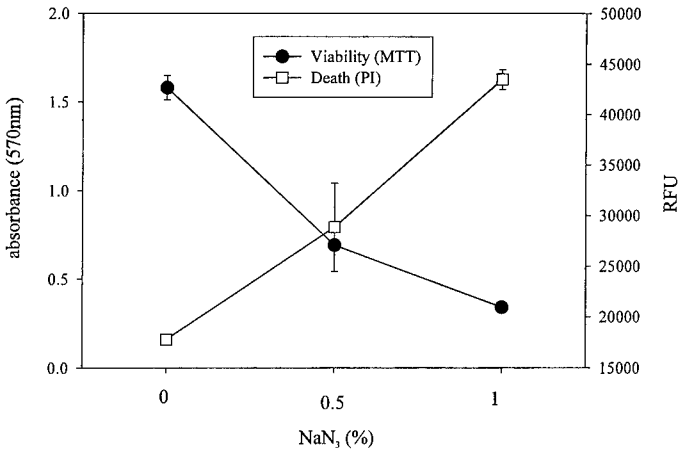

FIG. 4. Propidium iodide fluorescence inversely correlates with MTT absorption. A sample of 120,000 MCF-10A cells was exposed to the indicated concentrations of sodium azide (NaN_3) for 1 h. Cell viability was measured by the MTT method (absorbance, left axis). Cell death was measured by incorporation of propidium iodide (PI) (RFU, right axis). Error is represented as the standard deviation of 16 wells.

DISCUSSION

Several screening strategies currently exist for the identification of cytotoxic compounds, such as the National Cancer Institute's *in vitro* anticancer drug discovery screen (24). While unregulated cell migration is a nefarious aspect of cancer progression and other pathological processes such as arthritic inflammation, no high-throughput methods exist to identify inhibitors of cell migration. This is largely because conventional migration assays require excessive manipulation that reduces throughput and thus precludes them from being used in large-scale screens for antimigration compounds. In addition to the transfilter, modified Boyden chamber assay presented here, other methods for measuring cell migration include two-dimensional assays that measure random, nondirectional movement on a flat surface and three-dimensional migration/invasion assays, where cells are seeded into or allowed to invade a gelatinous matrix. We chose to use the transfilter migration assay based on the modified Boyden chamber for ease of use and simple determination of migrated vs nonmigrated cells.

In traditional Boyden chamber filter migration and invasion assays, the migratory or invasive cells are fixed, stained, and counted visually under a microscope. In this procedure, only representative fields are chosen and counted, a process that introduces operator bias. In order to discern migratory from nonmigratory cells in these assays, nonmigratory cells must be physically removed from the upper surface of the membrane. Aside from adding extra manipulation into the assay, the assessment may only be performed once, and it is difficult to assay viability of the removed cells. Cell quantification by fluorescence detection accounts for the fluorescence contribution of every cell, thus omitting operator variability. Other protocols for simplifying the quantification of migrated cells in a modified Boyden chamber apparatus use markers of cell number that are detected after the migrated cells have been lysed. These markers include radioactivity of cell lysate from ^{51}Cr-labeled cells (25), enzyme activity (26), and absorption of a cellular dye (27). Martin *et al.* (28) introduced a protocol for measuring neutrophil migration that also uses calcien-AM for the rapid and sensitive detection of migratory cells. While their protocol takes advantage of a high-throughput format (Neuro Probe, Gaithersburg, MD), this plate does not have a fluorescence-opaque filter, thus requiring that nonmigratory cells be scraped from the filter before quantification. Ours is the only protocol designed for the detection of cancer cell migration that incorporates both cell death and migration measurements of the same test cell population in the same assay.

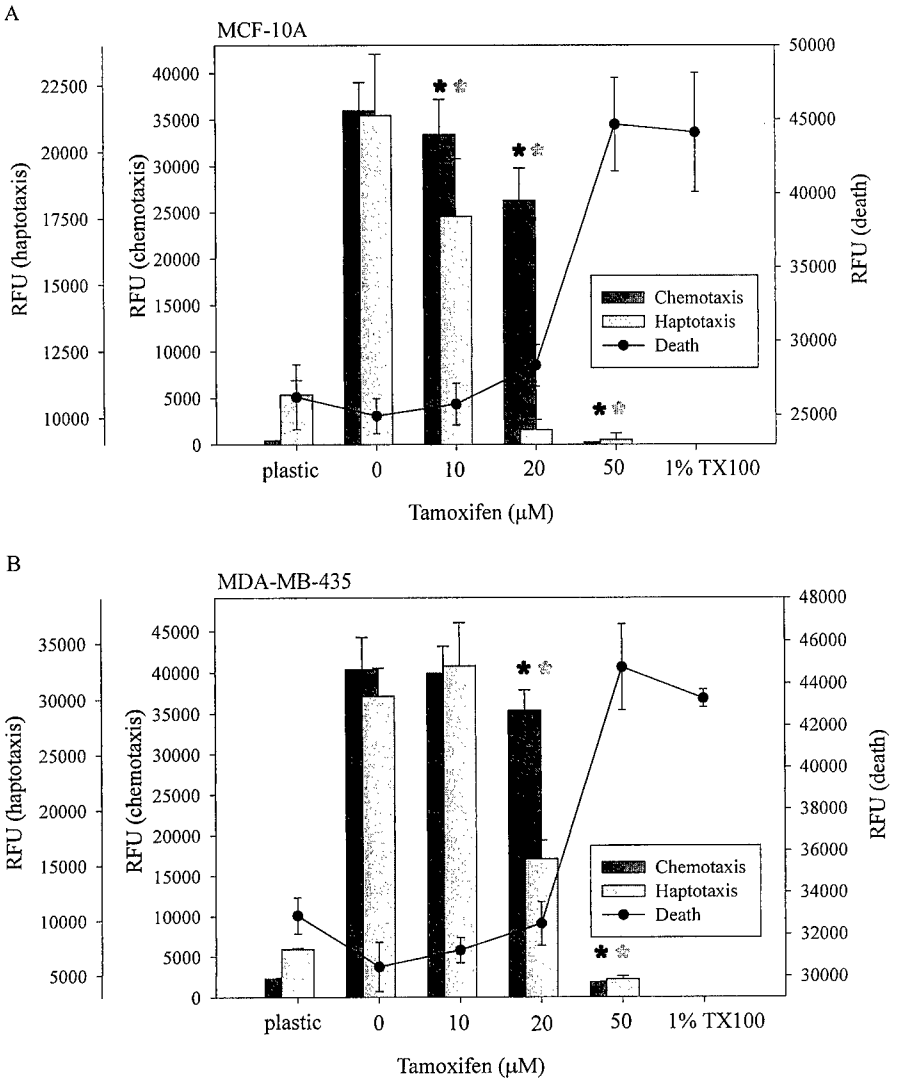

FIG. 5. MCF-10A (A, C) and MDA-MB-435 cells (B, D) were allowed to migrate toward serum (chemotaxis) or fibronectin (haptotaxis) in the presence of tamoxifen (A, B) or CAI (C, D). After 18 h, migrated cells were labeled with calcein-AM and fluorescence quantitated from the bottom. Nonmigrated cells were labeled with propidium iodide and fluorescence quantitated from the top. Estimation of 100% cell death was made by lysing cells in a filter well with 1% Triton X-100 (TX 100). Error bars represent the standard deviation of 4–16 replicate wells. Asterisks represent a significant difference from migration without drugs ($P < 0.05$).

Typical plates designed for transfilter migration assays are capable of handling only 12–24 samples each. Improvements to this design presented in this protocol have made the Boyden chamber easier and faster to use. These improvements include increasing the numbers of test chambers per plate, decreasing the size of the test chambers, and constructing all of the test chambers as one piece, so that all samples per plate can be handled simultaneously.

The complexity of signaling cascades regulating migration indicates that many different strategies can be exploited to disturb the stimulation of migration. The ability to migrate through the tissues of the body is a complicated process, involving tissue remodeling, directed movement, and arrest at sites of action (1). Aside from being an integral aspect of cancer metastasis, cell migration also plays an important role in normal cellular processes such as embryonic development, wound healing, angiogenesis, and the immune response. Each step is tightly regulated in normal tissues and involves the coordination of signals from extracellular matrix receptors, primarily integrins, and growth factor receptors (10, 29). The controls regulating cell movement, while incompletely understood, are diverse and vary among cell type. Compounds identified by this assay could affect any one of those processes, and identifying the mechanisms of action of those compounds could help clarify how cell migration is accomplished.

In this report, we demonstrate that tamoxifen, an antiestrogen that competes with estrogen for binding

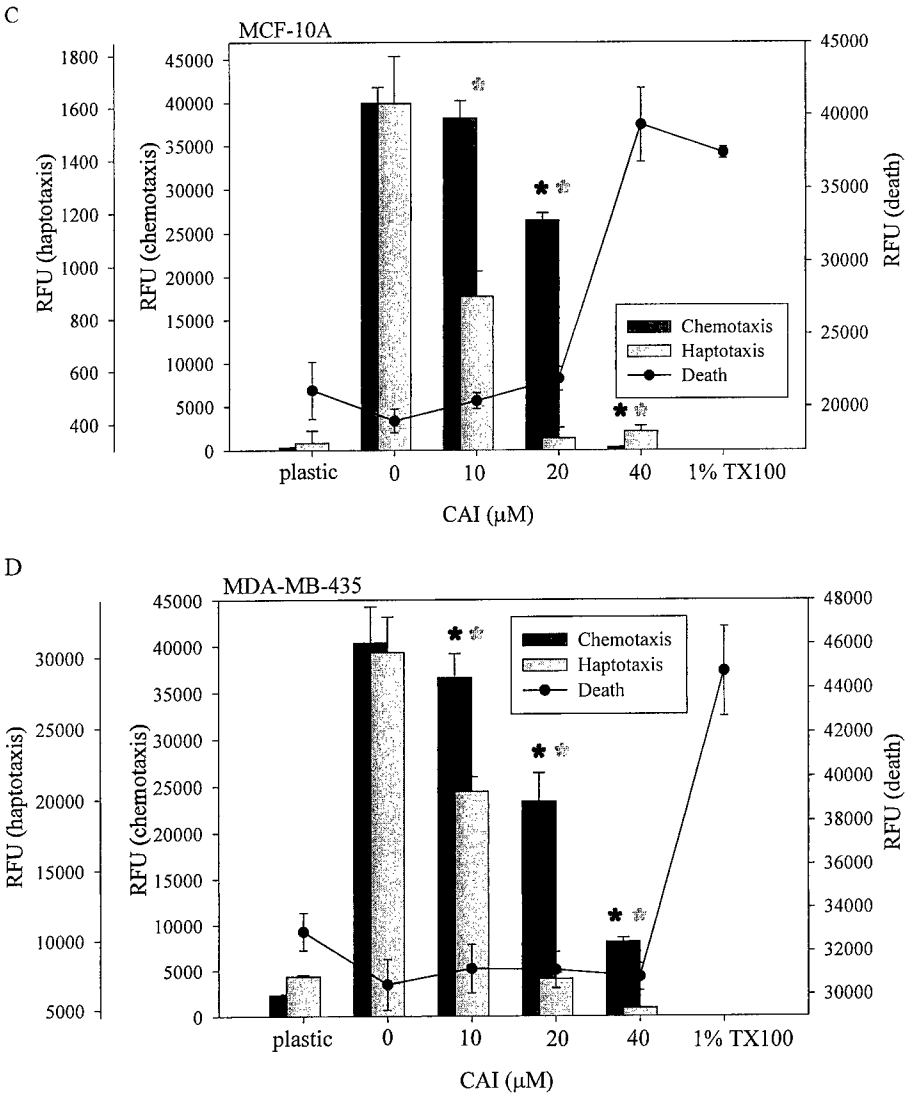

FIG. 5—*Continued*

the estrogen receptor (ER) (30), inhibits migration and causes cell death of ER-negative (MDA-MB-435) and ER-positive (MCF-10A) cells. This effect is not surprising since tamoxifen is shown to have an alternate mechanism for affecting antiproliferation and cytotoxicity, besides binding the estrogen receptor. In fact, ER-negative cancer patients can respond to tamoxifen while ER-positive patients can be insensitive (31). ER-negative breast cells, including MDA-MB-435 cells, have also been shown to respond to tamoxifen *in vitro* (31, 32).

The use of a fluorescence-blocking membrane suggests the possibility of measuring cell migration over time, as opposed to strictly endpoint analysis. We attempted to measure the decrease in fluorescence from the top of the filter plate and extrapolate those RFU measurements to cell number by comparison to a standard distribution of cells contained in wells of the same plate. To achieve this, the cells would have to be prelabeled with a bright, stable dye that did not influence cell migration patterns. We assessed four classes of live-cell fluorescent dyes for these properties, calcein-AM, SP-DiOC$_{18}$(3), CellTracker Blue, and carboxylate-modified fluorescent polystyrene microspheres (all purchased from Molecular Probes). Calcein-AM is a low-affinity calcium chelator (23) and inhibits migration of our cell lines, probably by interfering with calcium signaling required for migration (data not shown). These data are not surprising, as release of calcium from intracellular stores and opening of calcium channels in the plasma membrane are a consequence of integrin binding and requisite for migration under certain conditions (11, 33, 34). SP-DiOC$_{18}$(3) is a lipophilic carbocyanine membrane probe that is highly fluores-

cent when incorporated into cell membranes (23). While adhesion and migration are dependent upon membrane integrity, we found that SP-DiOC$_{18}$(3) did not influence migration and only subtly influenced adhesion in our cell lines (data not shown). While this dye showed promise, it exhibited less intense emission than calcein-AM and thus produced less sensitive results. In addition, while the fluorescence of this dye persisted throughout the migration assay, we found fluctuations in emission that interfered with results and were not readily explained. These fluctuations could be due to turnover of the cell membrane during the course of the assay or inherent limitations of the plate reader. CellTracker Blue is a cell-permeant thiol-reactive probe thought to produce fluorescent-glutathione adducts (23). This dye lacked the emission intensity required for these studies (data not shown). Carboxylate-modified fluorescent polystyrene microspheres offer another option for labeling migratory cells in a kinetic assay. These microspheres were spontaneously endocytosed and retained in the cytoplasm in our cell lines and do not interfere with invasion *in vivo* (35). In our assays, however, carboxylate microsphere labeling demonstrated poor reliability and sensitivity, perhaps by being processed and exocytosed from the cells before completion of the migration assay (data not shown). While these dyes are very effective in applications such as fluorescence microscopy where individual cells are visualized, they were not effective for quantifying large cell populations in kinetic migration assays.

In summary, we introduce a fluorescence-based, high-throughput assay for screening potential antimigratory compounds. With the use of two fluorescent indicators, this assay is designed to discern between cytotoxic and noncytotoxic mechanisms of action of migration-inhibiting compounds. Using this assay, we demonstrated that both the experimental anticancer compound CAI and the common breast cancer treatment tamoxifen inhibited cell migration at subcytotoxic concentrations. While MDA-MB-435 cells showed some resistance to cell death induced by high concentrations of CAI, CAI was more effective than tamoxifen at halting migration of both cell lines.

ACKNOWLEDGMENTS

We thank Dr. Nancy Chung-Welch, Becton Dickinson (Bedford, MA), for kindly providing 24-well fluorescence-blocking migration plates. We thank Dr. Elise C. Kohn, Laboratory of Pathology, National Cancer Institute, National Institutes of Health (Bethesda, MD), for kindly providing CAI. We also extend special thanks to Dr. Stephen W. Carper for critical reading of the manuscript and to Kilpatrick Carroll for technical assistance. This research was supported by grants from the U.S. Army (DAMD17-98-8325, to G.E.P.) and the UNLV office of sponsored programs.

REFERENCES

1. McKinnell, R. G., Parchment, R. E., Perantoni, A. O., and Pierce, G. B. (1998) *in* The Biological Basis of Cancer, pp. 14–28, Cambridge Univ. Press, Cambridge, UK.
2. Tannock, I. F., and Hill, R. P. (1992) *in* The Basic Science of Oncology (Tannock, I. F., and Hill, R. P., Eds.), pp. 302–337, McGraw-Hill, New York.
3. Kohn, E. C., and Liotta, L. A. (1995) Molecular insights into cancer invasion: Strategies for prevention and intervention. *Cancer Res.* **55,** 1856–1862.
4. Kee, J. L., and Hayes, E. R. (1997) *in* Pharmacology, a Nursing Process Approach, pp. 408–422, Saunders, Philadelphia.
5. Hahnfeldt, P., Panigrahy, D., Folkman, J., and Hlatky, L. (1999) Tumor development under angiogenic signaling: A dynamical theory of tumor growth, treatment response, and postvascular dormancy. *Cancer Res.* **59**(19), 4770–4775.
6. Gruninger, L., Cottin, E., Li, Y. X., Noel, A., Ozsahin, M., and Coucke, P. A. (1999) Sensitizing human cervical cancer cells *in vitro* to ionizing radiation with interferon beta or gamma. *Radiat. Res.* **152**(5), 493–498.
7. Guerra-Vladusic, F. K., Scott, G., Weaver, V., Vladusic, E. A., Tsai, M. S., Benz, C. C., and Lupu, R. (1999) Constitutive expression of heregulin induces apoptosis in an erbB-2 overexpressing breast cancer cell line SKBr-3. *Int. J. Oncol.* **15**(5), 883–892.
8. Lode, H. N., Moehler, T., Xiang, R., Jonczyk, A., Gillies, S. D., Cheresh, D. A., and Reisfeld, R. A. (1999) Synergy between an antiangiogenic integrin alphav antagonist and an antibody–cytokine fusion protein eradicates spontaneous tumor metastases. *Proc. Natl. Acad. Sci. USA* **96**(4), 1591–1596.
9. Price, J. T., Bonovich, M. T., and Kohn, E. C. (1997) The biochemistry of cancer dissemination. *Crit. Rev. Biochem. Mol. Biol.* **32**(3), 175–253.
10. Matsumoto, K., Ziober, B. L., Yao, C., and Kramer, R. H. (1995) Growth factor regulation of integrin mediated cell motility. *Cancer Metastasis Rev.* **14,** 205–217.
11. Lester, B. R., and McCarthy, J. B. (1992) Tumor cell adhesion to the extracellular matrix and signal transduction mechanisms implicated in tumor cell motility, invasion and metastasis. *Cancer Metastasis Rev.* **11,** 31–44.
12. Bauer, K. S., Figg, W. D., Hamilton, J. M., Jones, E. C., Premkumar, A., Steinberg, S. M., Dyer, V., Linehan, W. M., Pluda, J. M., and Reed, E. (1999) A pharmacokinetically guided Phase II study of carboxyamido-triazole in androgen-independent prostate cancer. *Clin. Cancer Res.* **5**(9), 2324–2329.
13. Lambert, P. A., Somers, K. D., Kohn, E. C., and Perry, R. R. (1997) Antiproliferative and antiinvasive effects of carboxyamido-triazole on breast cancer cell lines. *Surgery* **122**(2), 372–379.
14. Wasilenko, W. J., Palad, A. J., Somers, K. D., Blackmore, P. F., Kohn, E. C., Rhim, J. S., Wright, G. L., Jr., and Schellhammer, P. F. (1996) Effects of the calcium influx inhibitor carboxyamidotriazole on the proliferation and invasiveness of human prostate tumor cell lines. *Int. J. Cancer* **68**(2), 259–264.
15. Yangguan, W., Palad, A. J., Wasilenko, W. J., Blackmore, P. F., Pincus, W. A., Schecter, G. L., Spoonster, J. R., Kohn, E. C., and Somers, K. D. (1997) Inhibition of head and neck squamous cell carcinoma growth in invasion by the calcium influx inhibitor carboxyamido-triazole. *Clin. Cancer Res.* **3,** 1915–1921.
16. Hupe, D. J., Behrens, N. D., and Boltz, R. (1990) Anti-proliferative activity of L-651,582 correlates with calcium-mediated regulation of nucleotide metabolism at phosphoribosyl pyrophosphate synthetase. *J. Cell. Physiol.* **144**(3), 457–466.

17. Kohn, E. C., Sandeen, M. A., and Liotta, L. A. (1992) *In vivo* efficacy of a novel inhibitor of selected signal transduction pathways including calcium, arachidonate, and inositol phosphates. *Cancer Res.* **52**(11), 3208–3212.
18. Kohn, E. C., Jacobs, W., Kim, Y. S., Alessandro, R., Stetler-Stevenson, W. G., and Liotta, L. A. (1994) Calcium influx modulates expression of matrix metalloproteinase-2 (72-kDa type IV collagenase, gelatinase A). *J. Biol. Chem.* **269**(34), 21505–21511.
19. Plopper, G. E., Domanico, S. Z., Cirulli, V., Kiosses, W. B., and Quaranta, V. (1998) Migration of breast epithelial cells on Laminin-5: Differential role of integrins in normal and transformed cell types. *Breast Cancer Res. Treat.* **51**(1), 57–69.
20. Rust, W., Kingsley, K., Petnicki, T., Padmanabhan, S., Carper, S. W., and Plopper, G. E. (1999) Heat shock protein 27 plays two distinct roles in controlling human breast cancer cell migration on laminin-5. *Mol. Cell. Biol. Res. Commun.* **1,** 196–202.
21. Nieminen, A. L., Gores, G. J., Bond, J. M., Imberti, R., Herman, B., and Lemasters, J. J. (1992) A novel cytotoxicity screening assay using a multiwell fluorescence scanner. *Toxicol. Appl. Pharmacol.* **115**(2), 147–155.
22. Goldberger, A., and Septak, M. (1998) A Fluorescence Blocking Membrane Insert Enhances Analysis of Cell Motility Assays, Technical Bulletin 428, Becton Dickinson, Bedford, MA.
23. Haugland, R. P. (1996) Handbook of Fluorescent Probes and Research Chemicals, Molecular Probes, Eugene, OR.
24. Grever, M. R., Schepartz, S. A., and Chabner, B. A. (1992) The National Cancer Institute: Cancer drug discovery and development program. *Semin. Oncol.* **19,** 622–638.
25. Capsoni, F., Minonzio, F., Ongari, A. M., and Zanussi, C. (1989) A new simplified single-filter assay for "*in vitro*" evaluation of chemotaxis of ^{51}Cr-labeled polymorphonuclear leukocytes. *J. Immunol. Methods* **120**(1), 125–131.
26. Somersalo, K., Salo, O. P., Bjorksten, F., and Mustakallio, K. K. (1990) A simplified Boyden chamber assay for neutrophil chemotaxis based on quantitation of myeloperoxidase. *Anal. Biochem.* **185**(2), 238–242.
27. Grotendorst, G. R. (1987) Spectrophotometric assay for the quantitation of cell migration in the Boyden chamber chemotaxis assay. *Methods Enzymol.* **147,** 144–152.
28. Frevert, C. W., Wong, V. A., Goodman, R. B., Goodwin, R., and Martin, T. R. (1998) Rapid fluorescence-based measurement of neutrophil migration *in vitro*. *J. Immunol. Methods* **213**(1), 41–52.
29. Howe, A., Aplin, A. E., Alahari, S. K., and Juliano, R. L. (1998) Integrin signaling and cell growth control. *Curr. Opin. Cell Biol.* **10,** 220–231.
30. MacGregor, J. I., and Jordan, V. C. (1998) Basic guide to the mechanisms of antiestrogen action. *Pharmacol. Rev.* **50**(2), 151–196.
31. Charlier, C., Chariot, A., Antoine, N., Merville, M. P., Gielen, J., and Castronovo, V. (1995) Tamoxifen and its active metabolite inhibit growth of estrogen receptor-negative MDA-MB-435 cells. *Biochem. Pharmacol.* **49**(3), 351–358.
32. Shen, F., Xue, X., and Weber, G. (1999) Tamoxifen and genistein synergistically down-regulate signal transduction and proliferation in estrogen receptor-negative human breast carcinoma MDA-MB-435 cells. *Anticancer Res.* **19**(3A), 1657–1662.
33. Clark, E. A., and Brugge, J. S. (1995) Integrins and signal transduction pathways: The road taken. *Science* **268,** 233–239.
34. Siegel, G., Malmsten, M., and Klubendorf, D. (1998) Tumor cell locomotion and metastatic spread. *Microsc. Res. Tech.* **43,** 276–282.
35. Luzzi, K. J., MacDonald, I. C., Schmidt, E. E., Kerkvlier, N., Morris, V. L., Chambers, A. F., and Groom, A. C. (1998) Multistep nature of metastatic inefficiency. *Am. J. Pathol.* **153**(3), 865–873.

11

Cell shape control and mechanical signalling through the cytoskeleton

WOLFGANG H. GOLDMANN, JOSÉ LUIS ALONSO, KRZYSZTOF BOJANOWSKI, CLIFFORD BRANGWYNNE, CHRISTOPHER S. CHEN, MARINA E. CHICUREL, LAURA DIKE, SUI HUANG, KYUNG-MI LEE, ANDREW MANIOTIS, ROBERT MANNIX, HELEN McNAMEE, CHRISTIAN J. MEYER, KEIJI NARUSE, KEVIN KIT PARKER, GEORGE PLOPPER, THOMAS POLTE, NING WANG, LI YAN, and DONALD E. INGBER

1. Introduction

For the past twenty years, our group has explored the possibility that cells and tissues use a form of architecture, known as 'tensegrity', to control their shape and to transduce mechanical signals into changes in biochemistry and gene expression (1–5). The importance of the tensegrity paradigm is that it predicts that the form and function of living cells are controlled through changes in mechanical interactions between cells and their underlying extracellular matrix (ECM) adhesions that, in turn, alter cytoskeletal and nuclear structure inside the cell (1–6).

Tensegrity structures gain their stability from continuous tension and local compression, much like a tent fabric stiffened by internal tent poles and external pegs (5). In contrast to conventional engineering models, which viewed the cell as a viscous cytosol surrounded by an elastic membrane, the tensegrity model assumes that the cell is a discrete (porous) mechanical network that requires prestress (internal tension) to fully stabilize itself. This model recognizes that the molecular elements of the cell are dynamic. However, it predicts that, at any instant in time, the entire cell will behave as if it were 'hard-wired' by a continuous series of molecular struts, cables, and ropes that stretch from specific adhesion receptors on the cell surface to physically couple to discrete contacts on the surface of the nucleus and from there to the chromatin and genes within (2–4, 7). In this type of structure, external mechanical signals would not be transmitted equally across all points on the cell surface, rather mechanical stresses should be preferentially transferred across specific transmembrane receptors that physically link the cytoskeleton to the ECM or to junctions on other cells (2, 6). Furthermore,

changes in the balance of forces transmitted through the cytoskeletal network should result in short- and long-range changes in molecular arrangements in the cytoskeleton and nucleus as well as associated alterations in thermodynamic and kinetic parameters that may influence cellular biochemistry (2, 4, 6). The tensegrity model, therefore, led to many testable predictions relating to how cells structure themselves as well as how they sense and respond to external mechanical signals.

Since this theory was first published, we have set out to systematically test these predictions. Because of the key roles of cell microarchitecture and mechanical forces in this model, this required that we develop entirely new experimental techniques that would allow us to control cell deformation independently of cell binding to growth factors or ECM as well as methods for applying controlled mechanical stresses to specific cell surface receptors. In this chapter, we describe these methods and briefly review new insights into cytoskeletal signalling and cell regulation that have emerged from these studies.

2. Application of techniques

2.1 Control of cell shape by varying extracellular matrix density

One of the fundamental predictions of the tensegrity model is that cell form and function are determined through *mechanical* interactions with the cell's ECM adhesions. The corollary to this is that cell shape, mechanics, and function should change if cell–ECM binding interactions are varied so as to prevent or promote cell distortion. Indeed, in early studies, we were able to show that the growth and differentiation of specialized cells (e.g. capillary endothelial cells, primary hepatocytes) can be controlled by altering the ability of the ECM substrate to resist cell tractional forces (8–10).

This was accomplished by varying the density of purified ECM molecules, such as fibronectin (FN), coated on otherwise non-adhesive, bacteriological plastic dishes, as described in *Protocol 1*. In these studies, the cells had to be cultured in serum-free medium to focus on effects of varying cell–ECM binding interactions, independently of exogenous matrix proteins that are found in high concentrations in serum (e.g. FN, vitronectin). When cells are plated on these dishes, cell spreading and growth increase in parallel as the ECM coating density is raised (8–10) (*Figure 1*). When spreading is restricted and growth suppressed, differentiation (e.g. tube formation by capillary cells, secretion of liver-specific proteins by hepatocytes) is concomitantly turned on (9, 10). This system has also been used to demonstrate shape-dependent control of cell contractility and mechanics in vascular smooth muscle cells (11). We are now using this as a model to analyse how changes in cell binding to ECM and concomitant alterations in cell shape modulate the intracellular

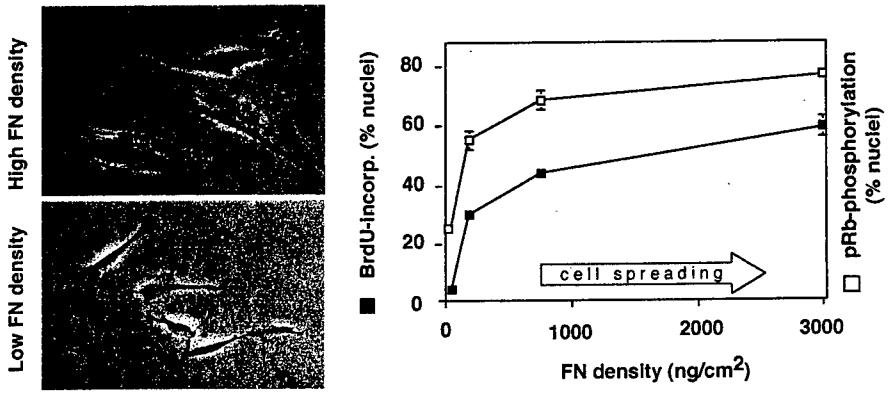

Figure 1. Modulation of cell shape. (*Left*) Phase-contrast view of human capillary endothelial cells plated on bacteriological dishes coated with high (*top*) and low (*bottom*) FN density. (*Right*) Cells plated on progressively higher FN density exhibit an increase in pRb phosphorylation and S phase entry as measured by nuclear BrdU incorporation. pRb phosphorylation was measured using *in situ* assay (12).

signalling cascade that controls this contractile response as well as cell cycle progression.

Protocol 1. Control of cell shape and function by varying ECM coating density

Equipment and reagents

- Bacteriological Petri dishes (Falcon Labware)
- 96-well plates (Immunolon II, Dynatech)
- Confluent cell monolayers
- Culture medium
- Lyophilized FN (Collaborative Biomedical Products, or Organon Teknika-Cappel, or Calbiochem)
- Carbonate buffer pH 9.4
- PBS
- 1% bovine serum albumin (BSA; Fraction V, Sigma)
- Trypsin-EDTA
- Serum-free media

Method

1. Two days prior to experiments, re-feed confluent cell monolayers with conventional culture medium containing low (0.5–1%) serum and no growth supplements in order to induce the cells to enter quiescence. Note: this may be difficult with transformed cells or certain cell lines. We have found that lovastatin provides an even more efficient method to synchronize cells in early G1 (12).
2. At least one day prior to experiment, resuspend purified ECM component, such as lyophilized FN in sterile distilled water (final concentration of 5 μg/ml) and store at 4°C. Allow 30–60 min for material to go into solution; do not pipette, agitate, or swirl. Note: similar results

Protocol 1. *Continued*

have been obtained with FN from multiple commercial sources. Store aliquots of lyophilized ECM molecules at –70 °C.

3. Dilute FN in carbonate buffer pH 9.4 to a final concentration that will add the required FN per well or dish in the following coating volumes: 100 μl/well in 96-well plates; 500 μl/24 mm dish, 5 ml/60 mm dish, 20 ml/100 mm dish, 30 ml/150 mm dish.
4. Incubate dishes overnight at 4 °C. Dishes can be stored for longer times in the cold prior to use. Cover tightly with Parafilm to minimize evaporation.
5. On the day of experiment, aspirate coating solution, wash twice with PBS, once with basal medium, and then block non-specific binding sites by incubating dishes in medium containing 1% BSA at 37 °C for at least 30 min.
6. While ECM-coated plates are sitting in medium containing 1% BSA, dissociate quiescent cell monolayers by brief exposure to trypsin-EDTA, collect by centrifugation, wash in medium containing 1% BSA to neutralize the trypsin, and plate cells on ECM-coated dishes in chemically-defined, serum-free medium. Note: use of serum to stop the trypsin will interfere with ECM-dependent control of cell shape and function; soybean trypsin inhibitor can also be added to ensure complete trypsin inactivation.
7. If the primary focus is on ECM-dependent control of cell shape and function, plate cells at a low density to minimize cell–cell contact formation in chemically-defined, serum-free medium containing 1% BSA. The exact composition of the medium will be dictated by the cell of choice. In certain cell types, such as capillary endothelial cells, higher plating densities are utilized when studies focus on control of ECM-dependent modulation of multicellular differentiation (e.g. capillary tube formation) (9).

2.2 Analysis of focal adhesion formation and integrin signalling

The results obtained with cells cultured on varying ECM densities demonstrated close coupling between cell spreading and growth (8–10), as demonstrated in past studies using other model systems (13). However, increasing the FN coating density does more than promote cell spreading, it also induces local clustering of cell surface ECM receptors, called integrins (14, 15). For this reason, it was necessary to develop methods to dissect out the biological effects induced by integrin clustering, independent of any associated cell shape change. We accomplished this by allowing round cells plated on a low FN density or suspended spherical cells to bind to small microbeads (4.5 μm

diameter) coated with a high density of FN, synthetic RGD-containing peptides, or specific anti-integrin antibodies (*Protocol 2*). Under these conditions, we could demonstrate that cells formed focal adhesion complexes (FACs) containing clustered integrins, talin, and vinculin, directly at the site of bead binding within 5–15 minutes after stimulation (16). In contrast, beads coated with a control ligand, acetylated-low density lipoprotein (AcLDL), bound to cell surfaces via transmembrane metabolic (scavenger) receptors but did not induce recruitment of any of these FAC proteins.

The rapid and synchronous induction of FAC formation obtained with this bead technique permitted an analysis of integrin signalling not possible with conventional methods. For example, we extended this work by using immunofluorescence microscopy to demonstrate that many signal transducing molecules that are turned on in response to binding to growth factor receptors as well as integrins (e.g. $pp60^{c\text{-}src}$, $pp125^{FAK}$, phosphatidylinositol-3-kinase, phospholipase C-γ, Na^+/H^+ antiporter, protein tyrosine phosphorylation) were also recruited to the cytoskeletal framework of the FAC in an integrin-specific manner and at similar times (17) (*Figure 2*). Finally, we took advantage of the fact that the beads we used were paramagnetic to develop a means to physically isolate these FACs away from the cell and remaining cytoskeleton (16, 17) (*Figure 3*; also see *Protocol 3*). Western blot analysis confirmed that FACs isolated using RGD-beads were enriched for $pp60^{c\text{-}src}$, $pp125^{FAK}$, phospholipase C-γ, and the Na^+/H^+ antiporter when compared with intact cytoskeleton or basal cell surface preparations that retained lipid bilayer. Isolated FACs were also greatly enriched for the high affinity fibroblast growth factor receptor. Most importantly, isolated FACs continued

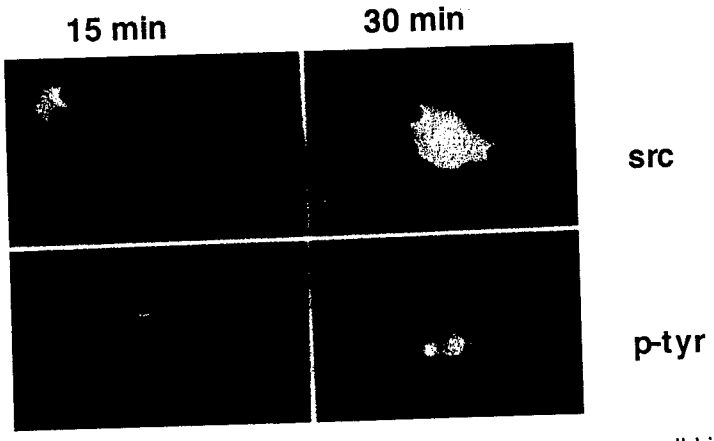

Figure 2. Recruitment of signalling molecules to the FAC in response to cell binding to FN-coated microbeads for 15 min (*left*) and 30 min (*right*). Positive immunostaining for src- and tyrosine-phosphorylated proteins is concentrated in a crescent-like pattern along the cell–bead interface.

1544

EM Analysis of the Spatial Distribution of Microtubules in Cultured Cells.

I.A. Alieva, O.A. Chernobelskaya, Y. A. Komarova, I.A. Vorobjev, Laboratory of Cell Motility

Two types of microtubules (MTs) could be observed in cultured cellswere: centrosomal (associated with the centrosome) and non-centrosomal (free cytoplasmic). Using 3D reconstruction based on the stereopairs of serial electron microscopic sections we examined the quantity and the lenght of MTs radiating from the centrosome and the average length of cytoplasmic MTs. The reconstruction of cytoplasmic MTs was undertaken after immunogold staning with antibodies against alpha-tubulin to differenciate the MTs from the other cytoskeleton components or after using procedure included consecutive fixations with tannic acid. The quantity of non-centrosomal MTs significantly exceeded the quantity of centrosomal MTs: almost 90% of cell MTs were free. Mean length of centrosomal MTs were similar in different cell lines (near 0,5 mm long). In the lamellum the mean length of MTs (2,5¦1,9 mm) exceedes the length of centrosomal. It has been shown that the longest MTs appeared to be in the thick layer of the cell lamella, predominantly under the cell nucleus (maximum length of MTs was 20 mm long), but such longest MTs were unnumerous. Above the lamella the MTs were shorter - not more than 10 mm, and in region of centrosome the maximum length was 4,5 mm long. The large standard deviation in the MTs length are consistent with the suggestion that both centrosome associated and cytoplasmic MTs are friquently nucleated and their elongation proceeds in a random (stochastic) way. The density of MTs in the cytoplasm determinated by EM is high enough to suggest that single MTs usually are not recognized as separate entities under the light microscope.

Molecular Biology (1545 - 1548)

1545

DNA detection with surface plasmon spectroscopy

Jianing liu, Max-Planck-Institute für polymerforschung, Ackermannweg 10, Mainz, D-55022

Now modern optical method have been broadly used in many biological molecular detection.We are focus on DNA detection with surface plasmon spectroscopy.With this technique,we can test both complimentary and mismatched DNA hybridization in a very less amount(25 micro litter),and a lower concentration(up to 1e-9M).The signal for DNA hybridization can be amplified with the formation of biomultilayer on the Au surface.This result has also been proved by fluorence spectroscopy.

1546

A High Throughput Assay for Screening Anti-Migratory Compounds

William L. Rust, Janice L. Huff, George E. Plopper, University of Nevada, Las Vegas

Large scale screening strategies aimed at finding anti cancer drugs traditionally focus on identifying cytotoxic compounds that attack actively dividing cells. Because progression to malignancy involves acquisition of an aggressively invasive phenotype in addition to hyperproliferation, simple and effective screening strategies for finding compounds that target the invasive aspects of cancer progression may prove valuable for identifying alternative and preventative cancer therapies. Here we describe a kinetic, fluorescence based automated assay for identifying anti-migratory compounds, with the ability to discern cytotoxic from non-cytotoxic modes of action. With this assay, we analyzed the experimental anti-cancer compound carboxy-amido triazole (CAI) and the common breast cancer treatment drug tamoxifen using the immortalized, but non-tumorigenic cell line MCF-10A, and the malignant breast cancer cell line MDA-MB-435. This technology lends itself to high-throughput screening and may be a valuable tool for future drug discovery.

1547

Transposon Mutagenesis in the Fission Yeast *Schizosaccharomyces pombe*

Ralf Behrens, Jacky Hayles, Paul Nurse, Imperial Cancer Research Fund, 44 Lincoln's Inn Fields, London, WC 2A 3PX

We have a major interest in understanding morphogenesis in the fission yeast *S. pombe*. Since many morphogenetic mutants are viable, the relevant genes cannot easily be cloned by complementation. In order to overcome this problem we want to develop a transposon mutagenesis system in fission yeast. This approach allows direct sequencing of the disrupted sequences, and rapid identification of the relevant genes from the *S. pombe* genome database. We have characterised the fission yeast retroposon Tf1 (1) further with regard to its suitability for insertional mutagenesis. Induction of transposition under different growth conditions showed a significant increase of transposition to 10%-20% in cells grown in log phase compared to under 5% for cells being kept in stationary phase. Analysis of Tf1 insertion sites by Southern blotting showed that 10% of the investigated mutants had double insertions. About 15% had a single insertion showing a similar pattern and the remaining 75% appeared to have a single random insertion. We investigated a potential target site specificity by determining the exact integration site of Tf1 in several mutants. Preliminary results suggest no specific target consensus sequence, however, integration appears to be biased towards intragenic regions. Currently we are using different screens based on positive selection in order to determine how efficient Tf1 disrupts open reading frames.

(1) Levin, H.L., Weaver, D.C., and Boeke, J.D., 1990, Mol Cell Biol, 10, 6791-6798

1548

Recombinational Cloning: A High-Throughput Gene Transfer Technology for Functional Analysis and Protein Expression.

James Hartley, Michael Brasch, Gary F. Temple, David Cheo, Deborah Polayes, Ray Harris, Robert Bebee, Diane Nelson, Weining Xu, Mai Dahmas, Kris Zuraitis, Andrea Long, Gary Gerard, Elizabeth Flynn, Dominic Esposito, Greg Endress, Maryann Rhodes, Joel Jessee, Life Technologies

As a result of numerous ongoing genome sequencing projects, large numbers of candidate open reading frames are being identified, many of which have no known function. The analysis of these genes typically involves transfer of various DNA segments into a variety of vector backgrounds for protein expression or functional analysis. We describe a method called Recombinational Cloning (RC) that uses *in vitro* site-specific recombination to transfer DNA segments between vector backbones. We present results that demonstrate the use of this approach for efficient, directional cloning of PCR products. Such cloned PCR products, or other DNA segments flanked by recombination sites, can then be "automatically" transferred into new vector backgrounds, simply by adding the desired "Destination" vector and recombinase. By incorporating appropriate selections, the desired subclones are recovered at high efficiency (typically >90%) following introduction into *E. coli*. The RC method is fast, convenient, and automatable, allowing numerous DNA segments to be transferred in parallel into many different vector backgrounds, in a single experiment. Resulting subclones maintain reading frame register, permitting the generation of amino and carboxy translation fusions. Approaches for optimization of protein expression, rapid functional analysis, and the integration of numerous technology platforms will be discussed.

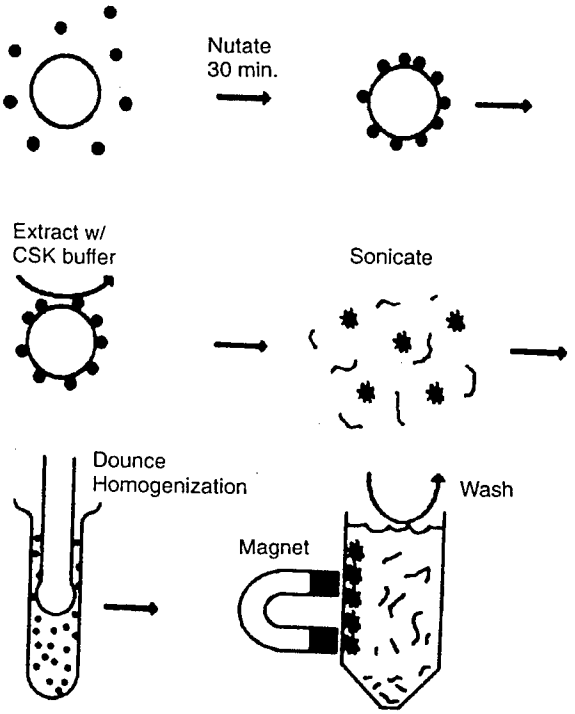

Figure 3. FAC isolation. Cells bound to RGD-coated beads were magnetically pelleted, extracted in CSK buffer, sonicated, and homogenized to remove nuclei and structures not intimately associated with the beads.

to exhibit multiple chemical signalling activities *in vitro*, including protein tyrosine kinase activities ($pp60^{c\text{-}src}$ and $pp125^{FAK}$) as well as the ability to undergo multiple sequential steps in the inositol lipid synthesis cascade (17, 18). This work, in combination with similar work from other laboratories (19), led to the realization that the FAC represents a major site for signal integration between growth factor and integrin pathways at the cell surface.

Protocol 2. Rapid induction of focal adhesion formation

Equipment and reagents

- Glass coverslips or slides (LabTek 8-well; Nalge NUNC International)
- Serum-free, chemically-defined medium
- Tosyl-activated magnetic microbeads (4.5 μm diameter; Dynal Inc.)
- 0.1 M carbonate buffer pH 9.4
- PBS
- 0.1% BSA
- Cytoskeleton stabilizing buffer (CSK–TX): 50 mM NaCl, 150 mM sucrose, 3 mM $MgCl_2$, 20 μg/ml aprotinin, 1 μg/ml leupeptin, 1 μg/ml pepstatin, 1 mM phenylmethylsulfonyl fluoride, 10 mM piperazine-*N,N'*-bis(2-ethanesulfonic acid) pH 6.8
- Triton X-100
- 4% paraformaldehyde

Method

1. Culture cells in serum-free, chemically-defined medium on glass coverslips or slides coated with a low FN density (e.g. 25–50 ng/cm^2) to hold cells in a round form and prevent spreading, using *Protocol 1*. This coating concentration may vary between different cell types and should be determined empirically.
2. Coat tosyl-activated magnetic microbeads (4.5 μm diameter) with ECM molecule, synthetic RGD peptide (Peptide 2000), specific antibodies, or control ligands, such as AcLDL (Biomedical Technologies Inc.) at 50 μg/ml in 0.1 M carbonate buffer pH 9.4 for 24 h at 4°C (15, 16). Coated beads are washed twice in PBS, incubated in medium containing 1% BSA for at least 30 min, and then stored at 4°C in PBS. Note: microbeads from Dynal or other suppliers that are pre-coated with secondary antibodies or other cross-linking agents may be used in a similar manner.
3. Add coated microbeads to cells (20 beads/cell) and allow to incubate for 5–30 min at 37°C.
4. To identify cytoskeletal-associated FAC proteins, incubate cells for 1 min in ice-cold cytoskeleton stabilizing buffer (CSK–TX) which maintains the integrity of the cytoskeleton (20). Incubate for 1 min in the same buffer supplemented with 0.5% Triton X-100 (CSK+TX) to remove membranes and soluble cytoplasmic components. Note: removal of soluble cytoplasmic contents also greatly increases the signal-to-noise ratio of FAC protein staining and may be advantageous for any study that focuses on morphological analysis of the FAC.
5. Fix detergent-extracted cells in 4% paraformaldehyde/PBS, wash with PBS, and incubate with primary antibodies diluted in 0.2% Triton X-100/0.1% BSA in PBS. Visualize primary antibodies using the appropriate affinity-purified anti-IgGFc antibodies conjugated to fluorescein or rhodamine (Organon Teknika-Cappel).

Protocol 3. Isolation of focal adhesion complexes

Equipment and reagents

- See *Protocols 1* and *2*
- Polypropylene tubes (Costar)
- 15 ml conical tubes (Falcon)
- Rotator (Nutator)
- Side pull magnetic separation unit (Advanced Magnetics)
- XL 2005 cell disruptor (Heat Systems)
- Dounce homogenizer (Wheaton)
- 1% BSA/DMEM
- CSK–TX and CSK+TX buffer (see *Protocol 2*)
- RIPA buffer: 1% Triton X-100, 1% deoxycholate, 0.1% SDS, 150 mM NaCl, 50 mM Tris pH 7.2, 0.1 mM AEBSF

Protocol 3. *Continued*

Method

1. Disperse quiescent cells with trypsin-EDTA as described in *Protocol 1*, wash with 1% BSA/DMEM, and place cells in polypropylene tubes.
2. Suspend approx. 10^6 cells/ml in defined medium without growth factors, add an equal volume of medium containing RGD-coated magnetic microbeads (2×10^7 beads/ml; coated as in *Protocol 2*), and place on a rotator for 30 min at 37 °C. RGD-coated beads are utilized because they exhibit less non-specific clumping in suspension than FN-beads, and thus allow greater binding efficiency. However, similar results have been obtained with FN-coated beads.
3. Use a side pull magnetic separation unit to collect microbeads and bound cells. This and all subsequent procedures are carried out at 4 °C.
4. Resuspend cell/bead pellet in ice-cold CSK–TX buffer and transfer these to 15 ml conical tubes.
5. Re-pellet using magnetic separator. Resuspend bead pellets in cold CSK+TX buffer (with detergent), incubate on ice for 5 min, sonicate for 10 sec (output setting, 4; output power, 10%), and homogenize (20 strokes) in a (100 μm) Dounce homogenizer.
6. Pellet microbeads magnetically and wash five times with 10 ml CSK+TX buffer. RIPA buffer is used to remove protein from beads for biochemical analysis.

2.3 Geometric control of cell shape and function

This finding that integrin clustering alone is sufficient to activate internal signal transduction pathways that can influence cell behaviour complicated the cell shape story. However, the cells that bound to these beads which induced integrin clustering and early signalling events, including expression of immediate early growth response genes (21), never entered S phase (8). Thus, we then set out to make cell shape or distortion an independent variable. In other words, we attempted to devise a system in which cells could bind to optimal densities of ECM and soluble growth factors, but yet could be restricted in their spreading by purely physical means.

To control cell deformation in this manner, we adapted a soft lithography-based micropatterning technique that was originally developed in Dr George Whitesides' laboratory at Harvard as an alternative manufacturing approach for the microchip industry (22, 23). This method allowed us to create ECM-coated adhesive islands with defined shape, size, and position on the micron scale that were separated by non-adhesive, polyethylene glycol (PEG)-coated boundary regions that do not support protein adsorption and hence, prevent cell adhesion. When cells are plated on these substrates they adhere and

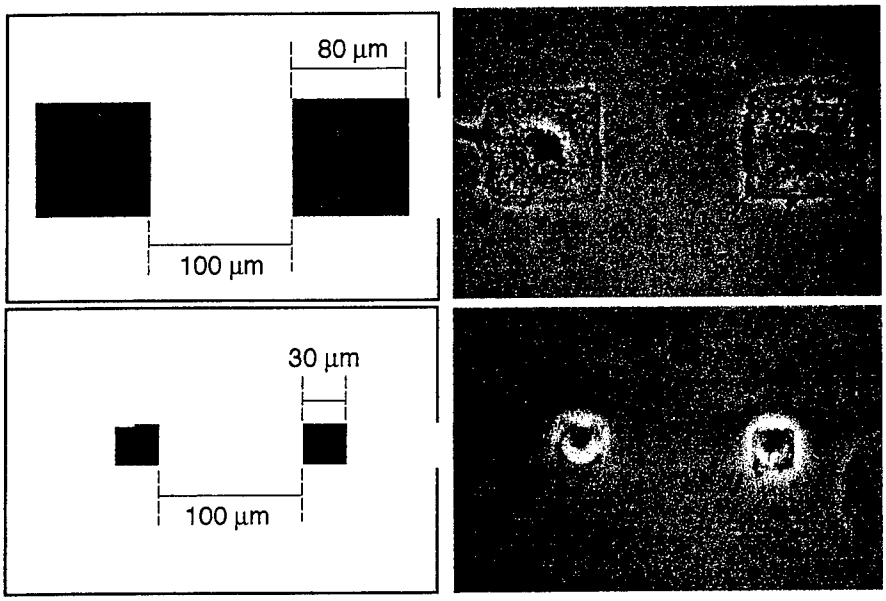

Figure 4. Control of human capillary endothelial cell shape using micropatterned substrates. Phase-contrast view (*right*) of CE cells plated on patterns containing FN-coated square islands 80 μm and 30 μm wide, respectively. The design of the pattern geometry is shown in the left panels, with the shaded area indicating the protein-adsorbing areas.

change their shape to fit the size and form of their container (i.e. of the patterned adhesive island) (24, 25) (*Figure 4*).

Methods for generating micropatterned substrates are described in *Protocols 4–8*. In brief, it involves a single photolithography step to generate a master etched pattern in silicon using a computer program commonly used for integrated circuit designs (23) (*Figure 5*). An elastomer (polydimethylsiloxane; PDMS) is then poured over the surface of this master and polymerized to form a 'rubber stamp' that retains the precise surface features of the micropattern down to less than 1 μm resolution. The outward facing features of the stamp are coated with a chemical 'ink' composed of alkanethiols. When the inked stamp is brought into contact with a gold-coated surface, the alkanethiols adhere tightly to the gold (Au) and self-assemble to form a space-filling monolayer that precisely fills the island form. A solution containing the same alkanethiol conjugated on its tail to a PEG blocking group is then poured over the slide surface. These alkanethiols self-assemble to fill all the spaces between the islands, creating a fully chemically-defined surface monolayer. However, because of the PEG blocking groups, ECM molecules will only adsorb to the surfaces of the islands when added in solution. This results in fabrication of highly adhesive, ECM-coated islands of defined shape, size, and position surrounded by non-adhesive, PEG-coated

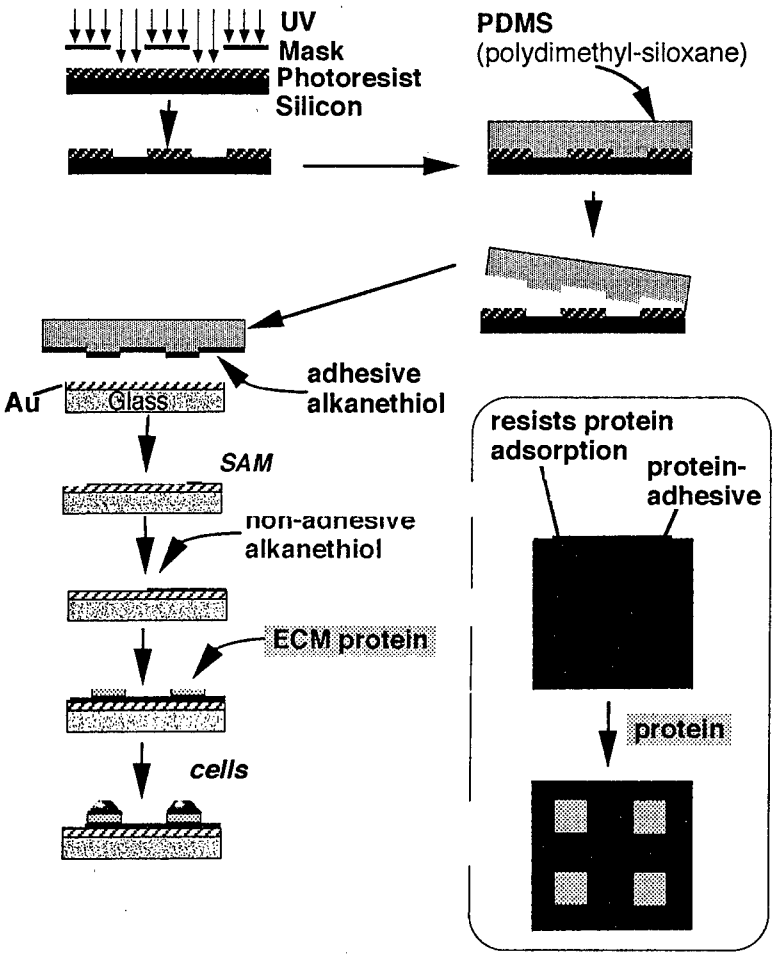

Figure 5. Schematic representation of the fabrication procedure for creating micropatterned substrates using microcontact printing. See text for details.

barrier regions. When cells are plated on these substrates they only adhere to the islands, spreading until they reach the surrounding non-adhesive boundary. By changing the size of the island, cells can be held in fully spread, moderately spread, or fully retracted form; by changing island form, cell shape can be controlled as well.

Using this micropatterning approach, we showed that capillary endothelial cells can be switched between growth, differentiation, and apoptosis programs simply by varying cell geometry (25, 26). For example, cells on large islands (50 μm diameter) that promoted cell extension supported growth, whereas cells on small islands (10 μm diameter) that remained fully retracted underwent a suicide program. To explore this mechanism, we allowed single cells to

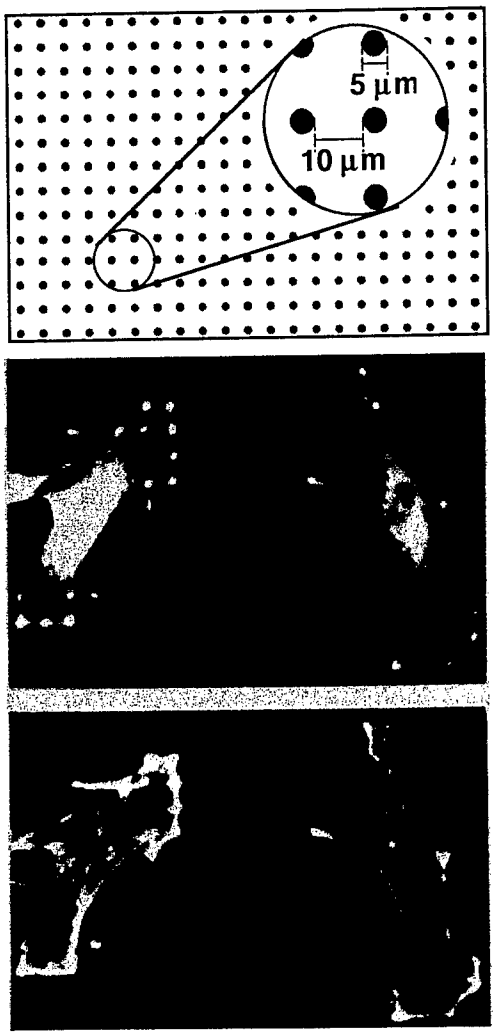

Figure 6. Micropatterns of 5 μm circles coated with fibronectin separated by 10 μm non-adhesive spaces (*top*), and immunofluorescence micrographs of adherent CE cells stained with anti-vinculin antibody (*middle*), and with FITC phalloidin (*bottom*) to visualize FACs and actin filaments, respectively.

spread across multiple, closely spaced, smaller adhesive islands that were the size of individual focal adhesions (3–5 μm diameter). Though the total area of these tiny islands was smaller than a single small (10 μm diameter) island, cells adherent to these patterned substrates spread as well as on a large island, stretching from island to island across non-adhesive areas (*Figure 6*). By increasing the spacing between islands, cell spreading could be increased by a

factor of ten without altering the total cell–ECM contact area. These observations revealed that cell shape—the degree to which the cell physically extends or retracts—governs whether cells grow or die (24). Most recently, using the same approach, we found that the motility of cells constrained on square adhesive islands is also controlled geometrically. Lamellipodia preferentially extend from the corners of these cells when stimulated with motility factors.

We are also using this micropatterning technique to expedite detection of focal adhesion-associated antigens in cells. Focal adhesion proteins commonly appear as small, spear-like streaks at the base of the cell when analysed by immunofluorescence microscopy. However, this is a highly subjective method and definitive characterization of a positively stained structure requires additional techniques, such as electron microscopy or interference reflection microscopy. By using substrates containing multiple focal adhesion-sized adhesive islands oriented in a regular pattern, we have overcome this limitation. Positive staining on these tiny islands represents antigens that are definitively concentrated in regions of cell anchorage to ECM and, hence, in focal adhesions. We are using this technique as a screening method, in conjunction with monoclonal antibody generation methods, to identify antibodies to novel focal adhesion proteins that may have structural or signalling roles relevant for cellular regulation.

Protocol 4. Generating a patterned silicon master using photolithography

Equipment and reagents

- Mask aligner (Karl Suss model)
- Silicon wafers
- Microscope
- Desiccator
- Trichloroethylene
- Acetone
- Methanol
- Hexamethyldisilazane (Shipley)
- 1813 positive photoresist (Shipley)
- (Tridecafluoro-1,1,2,2,-tetrahydro-octy)-1-trichlorosilane (United Chemical Technologies)

Method

1. Clean silicon wafers in a clean room (preferably Class A) by sonicating for 5 min successively in trichloroethylene, acetone, and methanol.
2. Heat wafers at 180°C for 10 min to dry thoroughly.
3. Spin coat (1500 g for 40 sec) the wafers with approx. 1–2 μm hexamethyldisilazane followed by a 1.3 μm thick layer of Shipley 1813 positive photoresist (1500 g for 40 sec).
4. Bake the resist at 105°C for 3.5 min.
5. Expose the wafer on a mask aligner through a photomask with features etched in chrome deposited on quartz (Advance Reproductions Corp.) for 5.5 sec at 10 mW/cm^2. The patterns on the

photomask are normally created on a glass plate coated with photosensitive emulsion using a pattern generator. The final film is made by contact printing of the emulsion plate onto the chromium-coated quartz plate.

6. Develop the features by immersing in Shipley 351 for 45 sec, then rinse with distilled water, and dry with a stream of nitrogen. The proper development of the features should be checked under a microscope using a red filter in front of the light source to avoid unwanted exposure of the photoresist.
7. Place the wafers in a desiccator under vacuum for 2 h. Use a vial containing 1–2 ml (tridecafluoro-1,1,2,2-tetrahydro-octy)-1-trichlorosilane that reacts with the silicon areas not covered by the photoresist and makes them hydrophobic. Rinse only with water and avoid all contact with organic solvents.

Protocol 5. Moulding elastomeric microstamps

Equipment and reagents

- Petri dishes
- Razor blade
- Polydimethylsiloxane (PDMS) (Sylgard 184, Dow Chemical Co.)

Method

1. Polydimethylsiloxane (PDMS) pre-polymer is made by mixing ten parts of monomer Silicone Elastomer-184 and one part of initiator Silicone Elastomer Curing Agent-184 thoroughly in a plastic container and degassing it under vacuum for approx. 1 h until air bubbles no longer rise to the top.
2. Pour the pre-polymer in a Petri dish that contains the patterned silicon wafer, and cure for at least 2 h at 60°C. Often small air bubbles form in the PDMS after it is poured on the master stamp. Cover the dish and gently tap it to allow the bubbles to diffuse out of the pre-polymer. Typically, stamps are 0.5–1 cm tall.
3. Peel the PDMS from the wafer and cut the stamps to the desired size with a razor blade. During curing, a layer of PDMS forms underneath the wafer and holds it to the dish. Invert the dish and gently press on the reverse side until the cured PDMS dewets from the surface of the dish. Invert the dish and use a dull edge to trace the contour of the PDMS so as to lift it off the dish. Often the PDMS remains attached to the wafer. Carefully cut the layer of PDMS found under the wafer and gently peel the two surfaces away from each other.

Protocol 6. Metal coating of glass substrates

Equipment and reagents

- Microscope slides (Fisher, No. 2)
- Electron beam evaporator
- Titanium (Aldrich, 99.99% purity)
- Gold (Materials Research Corporation, 99.99% purity)

Method

1. Load microscope slides on a rotating carousel in an electron beam evaporator (most of these are home-built).
2. Perform evaporation at pressure $< 1 \times 10^{-6}$ Torr. Occasionally, during the evaporation of titanium, the pressure increases above 1×10^{-6} Torr, but decreases after allowing the chamber to stabilize for approx. 2 min. Note: a sputter coat system also may be used to prepare these coatings. However, we recommend using an evaporator to coat the substrates because most sputter coaters are single source and, thus, they are impractical for coating two different metals (Ti and Au) on a single substrate. In addition, sputtering gives less homogeneous films that require an additional annealing step. Sputtering systems also generally produce films with higher quantities of metal oxides and other impurities that could interfere with the generation of the self-assembled monolayer (SAM) surface.
3. Allow the metals to reach evaporation rates of 1 Å/sec.
4. Allow 400–500 Å of each metal to evaporate before opening the shutters and exposing the glass slides to 15 Å of titanium (99.99% purity) followed by 115 Å of gold (99.99% purity).

Notes on storage: typically, gold-coated substrates become 'mottled' after four to five weeks and are no longer deemed suitable for experiments; streaks with heterogeneous transparency develop (they are obvious to the naked eye). This may be caused by rearrangements in the thickness of the gold layer related to impurities present on the glass before evaporation of the gold. Gold substrates that are stamped immediately after evaporation are generally more stable over time (approximately three months), perhaps because the SAM acts as a resist against impurities.

Protocol 7. Stamping micropatterned adhesive substrates

Equipment and reagents

- Q-tips
- Forceps
- Pasteur pipette
- Gold-coated substrate
- PDMS stamp
- 2 mM solution of hexadecanethiol ($HS-(CH_2)_{15}CH_3$) (Aldrich) in ethanol
- 2 mM PEG-terminated alkanethiol: tri(ethylene glycol)$HS(CH_2)_{11}(OCH_2CH_2)_3OH$ (synthesized at Dr G. Whitesides' laboratory)

Method

1. Lay metal-coated substrate on clean flat surface, with gold facing upward. Take care not to scratch the surface with sharp forceps, or to place the substrate upside down. If there is dust visible on the substrate, blow gently with pressurized air or nitrogen.
2. Rinse the PDMS stamp with ethanol and remove the ethanol vigorously with a stream of pressurized air or nitrogen for at least 10 sec. If any dust remains on the stamp, repeat this procedure.
3. Dip a Q-tip into a 2 mM solution of hexadecanethiol in ethanol and gently paint a layer of the solution onto the PDMS stamp. Use a stream of air or nitrogen to gently evaporate the ethanol off the stamp.
4. Gently place the stamp face down onto the gold-coated substrate and allow it to adhere; this step may require gentle pressure. Let the fully adhered stamp remain on the substrate for at least 10 sec. Observe the light reflected from the micropatterned substrate at an angle to ensure that the stamp has fully adhered to the substrate. A pink colour will ensure that full adhesion has occurred. Both under-stamping and over-stamping results in a loss of this interference pattern. Make sure that no patches of non-adhesion remain.
5. Use forceps to gently peel away the stamp from the substrate, making sure not to move the stamp against the substrate or to let the stamp re-adhere to the substrate.
6. Return to step 2 to continue stamping more substrates. After all substrates are stamped, proceed with step 7.
7. Use a Pasteur pipette to deliver an ethanol solution containing 2 mM PEG-terminated alkanethiol [tri(ethylene glycol)$HS(CH_2)_{11}(OCH_2CH_2)_3OH$] dropwise onto each substrate until the liquid covers it entirely. This usually requires approx. 0.5–1 ml per square inch of substrate. Incubate with the PEG-alkanethiol for 30 min to fill in the remaining bare regions of gold and complete the self-assembled monolayer surface coating. Note: always stamp the hexadecanethiol, rather than the PEG-alkanethiol. Stamping the PEG-alkanethiol results in less efficient pattern transfer, incomplete formation of the self-assembled monolayer, and non-specific adsorption of proteins in the 'non-adhesive' PEG-coated barrier regions.
8. With forceps—cleaned with ethanol and blown dry—grasp the corner of the substrate and rinse with a stream of ethanol on both sides of the pattern for 20 sec. Place the substrate on a clean surface and rinse the forceps with ethanol. Grasp the substrate again in a different location and rinse with ethanol to wash the area previously masked by the forceps.

Protocol 8. *Continued*

9. Blow off ethanol from the substrate with pressurized air or nitrogen.
10. Place the stamped substrates into containers, taking care not to allow the patterned surface to rub against any coarse surfaces. Store under nitrogen gas in a cool, dark location. Place the containers in a Ziplock bag filled with nitrogen.

Notes on storage: typically, alkanethiols kept in ethanolic solutions for more than three months become oxidized and form significant amounts of disulfides. Disulfides of PEG are detected by TLC as spots with an R_f of approximately 0.15, while the thiol has an R_f of 0.25 using CH_2Cl_2:CH_3OH (98:2) as the eluent. By NMR, disulfides can be distinguished from alkane thiols by the presence of a triplet of peaks (from the methylene group adjacent to the sulfur atom) at approximately 2.6 p.p.m. instead of a quartet at 2.5 p.p.m. Although disulfides are known to form SAMs with interfacial properties similar to those formed with alkanethiols, their assembly is 7 times slower.

Protocol 8. Culturing cells on micropatterned substrates

Equipment and reagents

- Petri dishes
- Microscope
- PBS
- ECM protein (25 μg/ml)
- 1% BSA dissolved in PBS
- Trypsin-EDTA
- 1% BSA/DMEM
- Serum-free media

Method

1. Prepare a solution of phosphate-buffered saline (PBS) containing the ECM protein (25 μg/ml) to be coated on the adhesive islands.
2. Place a small droplet (0.25 ml) of ECM solution onto a bacteriological Petri dish or another disposable hydrophobic surface that is non-adhesive for cells in the absence of serum. Typically, 0.25 ml of solution per square inch of substrate is sufficient. Float each substrate, with patterned side face-down, on the drops. Let sit for 2 h at room temperature.
3. After 2 h, add a large amount (5–15 ml) of 1% BSA dissolved in PBS directly to the dish in order to dilute the ECM protein solution and block further coating. Remove the substrates, flip the slide so that micropattern side is facing-up, and place directly into serum-free medium containing 1% BSA. Note: when adding the BSA/PBS solution, the slides can sink onto the dish and adhere to it; since the substrates face the bottom of the dish, the pattern may be damaged.

To avoid this, gently add the BSA solution around the edges of the substrate so that the slides remain afloat.

4. Dissociate quiescent cell monolayers by brief exposure to trypsin-EDTA, wash, and resuspend in 1% BSA/DMEM, as described in *Protocol 1*. Remove one-half volume of 1% BSA/DMEM from Petri dishes containing the micropatterned substrates and replace with an equal volume of medium containing cells at a low plating density (e.g. 7500 cells/cm^2) plus any required medium supplements at twice the concentration. Note: if serum-containing medium must be utilized, initially plate cells for at least 1 h in serum-free medium (this may only be necessary for certain cell types). Subsequent medium changes should minimize drying, which can non-specifically adsorb medium proteins onto the substrate and thus, compromise shape control. We commonly remove 75–90% of the old medium and replace it with new at each refeeding rather than remove all fluid during these medium changes. Note: a low cell plating density is utilized to optimize plating of single cells on individual islands and because the actual surface area available for cell adhesion on the patterned slides is a fraction of that of a regular culture dish. The cell plating densities and medium conditions will vary between different cell types and thus, should be determined empirically.
5. Visualize cells by any standard microscopic technique when micropatterning is performed on glass slides. Immunofluorescence staining of cytoskeletal and FAC components may be performed as described in *Protocol 2*.

2.4 Analysis of transmembrane mechanical signalling

The tensegrity model predicts that ECM regulates cell shape and function based on its ability to balance cytoskeletal tension that is transmitted across discrete transmembrane adhesion receptors on the cell surface. To analyse the molecular mechanism by which cells transfer external mechanical signals across the cell surface and to the cytoskeleton, we developed a magnetic twisting device (magnetic cytometry system) in which controlled mechanical stresses can be applied directly to specific subclasses of receptors on the surface of living cells (27, 28). In this technique, cultured cells are allowed to bind to small ferromagnetic beads coated with specific receptor ligands, as described in *Protocol 2*. Shear stress (torque) is applied to the membrane receptor-bound ferromagnetic microbeads by magnetically twisting the beads. This is accomplished by first magnetizing the beads by applying a very brief, but strong, homogeneous magnetic field in the horizontal direction. Then a weaker, but sustained magnetic field is applied in the vertical direction. This does not remagnetize the beads; instead, the beads realign along the new

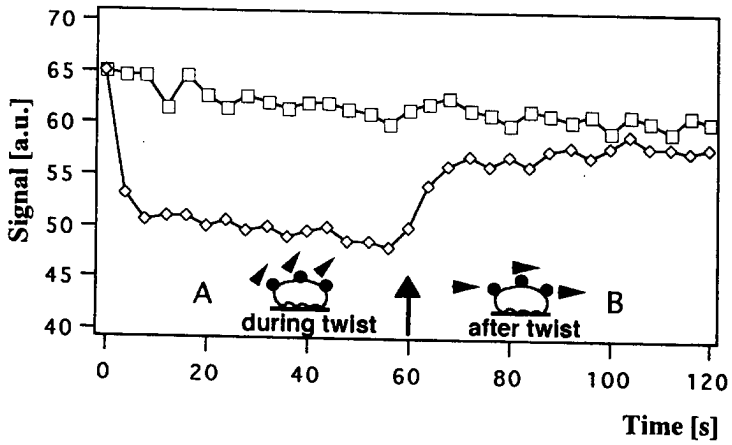

Figure 7. Data obtained using magnetic twisting cytometry showing the magnetic signal in the absence (squares) and presence (diamonds) of the twisting field. Application of a constant twisting stress (40 Gauss) for 60 sec in the vertical direction results in an instantaneous decrease in the signal. The difference in signal (on/off) at 60 sec is used to calculate the apparent stiffness, *E*. The rate of recovery after 60 sec multiplied by *E* determines the apparent viscosity (see *Equation 1*).

applied field lines much like a compass needle. Thus, the cellular response to applied stress can be measured simultaneously by quantifying changes in the rate and degree of magnetic bead rotation (i.e. angular strain) using an in-line magnetometer (*Figure 7*). This method is described in *Protocol 9*. Note: ferromagnetic beads must be used in these studies because, in contrast to the paramagnetic beads we utilized in our FAC isolation procedure, these materials must maintain their magnetization when an applied magnetic field is removed.

The values of the material properties measured using this technique will vary depending on the cell surface receptor to which that force is applied. Thus, this method allows one to measure micromechanical behaviour of different molecular supporting frameworks in the cell. When force is applied through cell surface integrins, the resulting shear stress is transmitted through the cell, causing the intracellular cytoskeleton to deform without producing large scale changes in cell shape (27). Using this technique, we showed that integrin receptors efficiently mediate mechanical force transfer across the cell surface through the FAC and to the cytoskeleton in endothelial cells and vascular smooth muscle cells, although different receptor subtypes varied in their response (integrin $\beta1 > \alpha Vb3 > \alpha5 > \alpha2 > \alpha V$) (11, 27–33). Other adhesion receptors, such as cadherins and selectins, mediated mechanical force transfer to the cytoskeleton to a moderate degree, whereas transmembrane receptors not involved in adhesion, such as metabolic scavenger

receptors and histocompatibility antigens, displayed minimal mechanical coupling (27, 31, 34). In addition, we consistently found that the stiffness (i.e. the ratio of stress to strain) of the cytoskeleton increased in direct proportion to the applied stress and thus, that the cytoskeleton behaves as a tensionally-integrated or 'tensegrity' structure (27).

Additional support for this model came from the finding that the mechanical stiffness at the cytoskeleton depended directly on the level of pressure (pretension) in the cytoskeleton (11, 30, 35).

We recently showed that the same magnetic twisting method can be used to analyse mechanochemical signalling in living cells. For this application, the magnetometer is used to verify the level of applied mechanical twisting stresses rather than to record experimental data. Changes in cellular biochemistry are measured simultaneously using conventional biochemical and molecular biological techniques. For example, magnetically twisting beads bound to cell surface integrins in adherent endothelial cells were found to induce recruitment of total poly(A) mRNA and ribosomes to the focal adhesions that form at the site of bead binding, as detected using high resolution *in situ* hybridization and immunofluorescence microscopy (36). Recruitment of the protein translation machinery was shown to be integrin-specific and dependent on the level of applied mechanical stress. These data suggest that altering the balance of mechanical forces, specifically across integrins, changes the intracellular biochemistry and, in this case, induces the formation of a microcompartment at the focal adhesion specialized for protein synthesis. Again, these results add experimental support for the predictions made by the tensegrity model. We are now using this method of localized stress application in cells expressing GFP-labelled cytoskeletal proteins (e.g. actin, tubulin, vinculin) to analyse directly how the cytoskeleton bears and distributes mechanical loads.

Protocol 9. Magnetic twisting cytometry

Equipment and reagents

- Spherical ferromagnetic beads obtained commercially (4.5 μm diameter, CFM-40-10 carboxylated-ferromagnetic beads; Spherotech) or from independent laboratories (1.4 μm or 5.5 μm diameter beads; Dr W. Moller, Gauting, Germany)
- Magnetic twisting device
- In-line magnetometer
- 96-well Removawells (Immunolon II)
- 100000 centipoise, PSAV100K (Petrarch Systems Inc.)

Method

When carboxylated-Spherotech beads are utilized, ligands are conjugated at 50 μg/ml using a carbodiimide (EDC; Sigma E-6383) reaction, as described by the supplier. The other beads are coated with adhesive ligands or antibodies at the same concentration, using methods described for paramagnetic Dynal microbeads in *Protocol 2*. Beads may also be

Protocol 9. *Continued*

obtained pre-coated with secondary antibodies (e.g. goat anti-mouse IgG Fc domain), to which can be added primary antibody in sterile PBS at 10–50 μg/ml (this concentration needs to be determined empirically for each antibody to ensure optimal binding). Store beads in sterile PBS at 4°C. Note: do not magnetically separate during washing steps because these beads will remain magnetized and thus, will be difficult to dissociate.

1. Plate cells (3×10^4/well) on FN-coated bacteriological plastic dishes (96-well Removawells) and culture for 6–10 h in chemically-defined medium before bead addition. The beads are quenched in chemically-defined medium containing 1% BSA for at least 30 min before being added to the cells.
2. Add approx. 1–10 beads/cell (this should be determined experimentally to obtain approx. 1–4 bound beads/cell) and incubate in chemically-defined medium containing 1% BSA for 15–30 min. At this time, the cells are washed in serum-free medium to remove unbound beads.
3. Place the individual well containing cultured cells and bound beads within a plastic vial, and then place it into the holder of the magnetic twisting device. Rotate at a constant rate (5 r.p.m.) to reduce ambient noise. The vial prevents the circulating water used for temperature control from getting into the culture well.
4. Apply a brief (10 μsec) but strong (1000 Gauss) magnetic pulse in the horizontal direction (parallel to the culture surface), using one pair of the magnetic coils of the device. After several seconds, apply a much weaker magnetic twisting field (0–40 Gauss) in the vertical direction and twist the beads for 1 min. The vertical field can be altered to assess the effects of force duration and frequency as well as the form of the stress regimen (e.g. square wave versus sinusoidal).
5. Use an in-line magnetometer to detect changes in the magnitude of the bead magnetic vector in the horizontal direction. Note: the torque of the applied twisting field is proportional to the twisting field, bead magnetization, and the sine of the angle between the twisting field vector and the bead magnetization vector (27). In the absence of force transmission across the cell surface, the spherical beads turn in place by 90° into complete alignment with the twisting field, and the remaining field vector immediately drops to zero. In contrast, transmission of force to the cytoskeleton results in increased resistance to deformation and decreased bead rotation. Angular strain (bead rotation) is calculated as the arc cosine of the ratio of remanent field after 1 min twist to the field at time 0.

6. Determine the apparent stiffness (ratio of stress to strain) and viscosity using the following relation:

$$E = \frac{\sigma}{\phi} \quad \text{and} \quad \eta = E\tau \qquad [1]$$

where E is the apparent stiffness; σ is the effective stress; ϕ is the angular rotation of the microbead; η is the apparent viscosity; and τ is the time constant of recovery after stress release. In the absence of the applied twisting field, the magnetic signal exhibits only a small decrease or relaxation in signal that is due to thermal motion and membrane movement. However, when a constant twisting field (e.g. 30 Gauss) is applied in the vertical direction for 1 min, the magnetic signal of the beads decreases almost instantaneously (to zero when the beads are free in solution). By subtracting the relaxation signal from the control, the remanent field signal almost reaches a plateau after 1 min. This plateau value obtained 1 min after stress application (representing magnetic torque being balanced by the elastic component of the cell) is used to calculate the apparent stiffness of the cell according to the above relation (*Figure 7*).

7. Quantitate the energy stored elastically in the cell by turning off the twisting field for 1 min and measuring the extent of recovery of the bead magnetic signal. The difference in the signal that remains after 2 min relative to the remanent field signal is a readout of permanent deformation.

8. Calibrate the effective applied stress by placing microbeads in a standard solution of known viscosity (e.g. 100 000 centipoise, PSAV100K) (28, 29) and measuring angular strain. The effective stress equals:

$$\sigma = cH_a \frac{B_{twist}}{B_{relax}} \; ; \; \phi = \cos^{-1}\left(\frac{B_{twist}}{B_{relax}}\right) \qquad [2]$$

where c is a constant dependent on the magnetic property of the bead:

$$c = v \times 1/T$$

where v is the standard viscosity; $1/T$ is the slope of *tan* $(90° - \phi/2)$ versus time; H_a is the applied twisting field; B_{twist} is the remaining twisting signal at 60 sec; B_{relax} is the remanent relaxation signal at 60 sec. Note: it is assumed that the angular rotation of the bead is a direct readout of the angular strain of the cell.

For studies on mechanochemical transduction, controlled stresses are applied in a similar manner, and biochemical or morphological changes are measured inside the cells using conventional analytical techniques. For example, cells plated on small ECM-coated coverslips can be bound to magnetic beads, twisted, fixed, and then analysed using *in situ* hybridization or

immunofluorescence microscopy (36). It is also possible to use this technique to twist large numbers (millions) of suspended cells bound to magnetic beads in order to measure biochemical changes inside the cells (e.g. cAMP levels). Larger numbers (10–20) of beads bound per cell may be utilized for these studies.

2.5 Detection of long-range mechanical signal transfer

The tensegrity model of integrated cell shape control assumes that transmembrane ECM receptors, cytoskeletal filaments, and nuclear scaffolds are 'wired' together in such a way that mechanical stimuli can change the organization of molecular assemblies deep in the cytoplasm and nucleus. This is contrary to many existing models which view the cell as a viscous cytoplasm surrounded by an elastic membrane that bears most of the mechanical load. We recently developed a microsurgical approach to demonstrate that living cells and nuclei are indeed hard-wired such that a mechanical tug on cell surface receptors can immediately change the organization of molecular assemblies in the cytoplasm and nucleus (37). Specifically, when integrins were pulled by micromanipulating bound ECM-coated microbeads or micropipettes, cytoskeletal filaments reoriented, nuclei distorted, and nucleoli redistributed along the axis of the applied tension field. These effects were specific for integrins, independent of cortical membrane distortion, and mediated by direct linkages between the cytoskeleton and nucleus.

We extended these studies to analyse long-distance stress transfer and connectivity in the cytoskeleton and the nucleus, by using a very fine microneedle (0.5 μm diameter) to 'harpoon' the cytoplasm at precise distances from the nucleus and then rapidly pulling it away from the nucleus, toward the cell periphery (37). Cells remained viable during this procedure. We used digitized image analysis and real-time video microscopy to determine the position of multiple phase-dense structures within the cytoplasm and the nucleus (e.g. mitochondria, vacuoles, nucleoli, nuclear envelope) before and after pulling the micropipette away from the nucleus using the micromanipulator. By harpooning the cytoplasm with uncoated micropipettes and applying stresses directly to the cytoskeleton in cells treated with different cytoskeleton-modulating drugs, we were able to show that actin microfilaments mediated force transfer to the nucleus at low strain; however, tearing of the actin gel resulted in greater distortion (37). In contrast, intermediate filaments effectively mediated force transfer to the nucleus under both conditions, and cell tearing resulted when intermediate filaments were disrupted either by pharmacological means (37) or using genetic recombination (38). Finally, by placing the pipette tip closer to the nuclear border (2–4 μm) or within the nucleoplasm itself and then pulling away from the nuclear envelope, we could demonstrate the presence of discrete (localized) sites of mechanical stress transfer between the cytoplasm and nucleus as well as between the nucleoplasm and the nuclear envelope (37) (*Figure 8*).

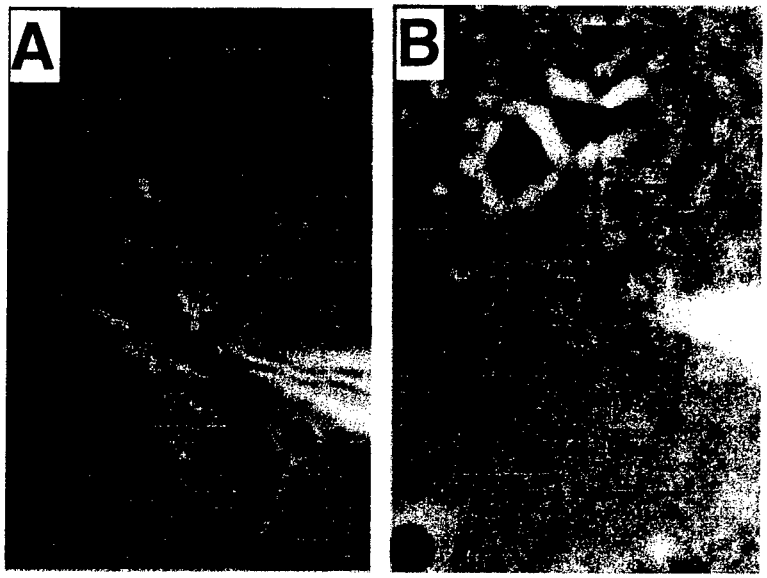

Figure 8. Demonstration of discrete connections between cytoskeletal and nuclear scaffolds. (A) A cell harpooned by a microneedle close to the nuclear border after stress application. The *arrow* indicates a local tongue-like protrusion of the nuclear envelope. (B) Invagination of the nuclear envelope in response to harpooning the nucleoplasm. Four small *arrows* indicate the tensed nucleoplasmic thread stretching from the pipette tip.

We also used the harpooning approach to estimate relative changes in mechanical stiffness of the cytoplasm and nucleus (37). The stiffness (E) of the cytoplasm and nucleus, as in any material, equals stress (s) (force/cross-sectional area) divided by strain (e) (change in length/initial length). The stiffness of the cytoplasm and nucleus cannot be determined directly using the harpooning technique, because only induced strains are measured. However, the ratio of stiffness in the cytoplasm (c) and nucleus (n) can be determined in the following manner (*Figure 9*). The ratio of nuclear to cytoplasmic stiffness (E_n/E_c) will equal the ratio of cytoplasmic to nuclear strain ($\varepsilon_c/\varepsilon_n$) measured in these regions when exposed to the same stress. If the cell responds isotropically and homogeneously to stresses applied over short (micrometre) distances, then the stress tensor (three-dimensional stress field) produced at any point will depend primarily on its location relative to the site of force application. Thus, the ratio of nuclear to cytoplasmic stiffness can be calculated by determining the ratio of induced strains measured in regions of the cytoplasm and nucleus when placed at the same distance from the micropipette (i.e. even if in different regions of the cell). We adapted the harpooning method to quantitate apparent Poisson's ratios as a measure of mechanical connectivity within the cytoplasm and nucleus of living cells.

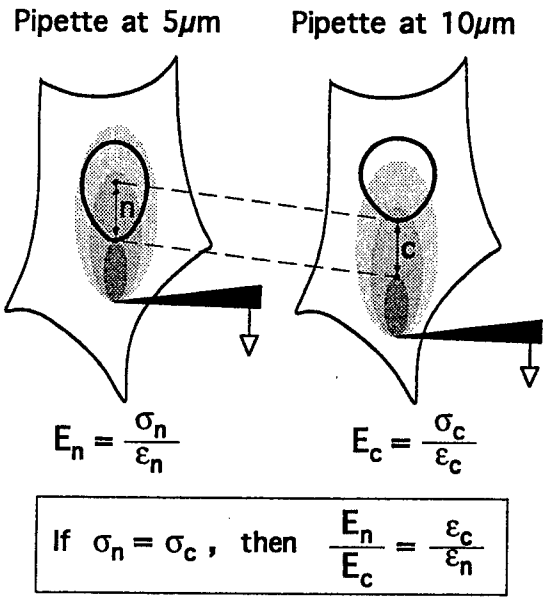

Figure 9. Schematic diagram demonstrating how relative changes in the mechanical stiffness of the cytoplasm and nucleus can be analysed in living cells.

Based on these studies, we found that intermediate filaments and actin filaments acted as molecular guy wires to mechanically stiffen the nucleus and anchor it in place, whereas microtubules acted to hold open the intermediate filament lattice and to stabilize the nucleus against lateral compression. Thus, these results added direct experimental support for our hypothesis that molecular connections between integrins, cytoskeletal filaments, and nuclear scaffolds may provide a discrete path for long-range mechanical signal transfer through cells as well as a mechanism for producing integrated changes in cell and nuclear structure in response to changes in ECM adhesivity or mechanics. Our methods for analysis of long-distance force transfer through the cytoskeleton as well as cytoplasmic and nuclear mechanics are presented in *Protocols 10* and *11*.

Protocol 10. Microsurgical analysis of long-range mechanical signalling

Equipment and reagents

- FN-coated glass coverslips
- Needles (Narishige)
- Pipette puller (Sutter)
- Manual micromanipulator (Leitz)
- Tosyl-activated microbeads (4.5 μm diameter; Dynal)
- Culture media

Method

1. Culture cells for 6–24 h in serum-free, chemically-defined medium containing 1% BSA on FN-coated glass coverslips. For studies involving force application to cell surface integrins, cells should be cultured on a suboptimal FN density (200–400 ng/cm^2) that promotes only a moderate degree of spreading, using the method in *Protocol 1*. Note: long-range distance transfer is difficult to visualize in well-spread cells on a high ECM density because these cells are too stiff, and most of the applied load is borne by their basal adhesions to the rigid ECM-coated substrate.
2. Pull needles with pipette puller and affix them to a manual micromanipulator. The micropipettes should be formed with tips approx. 0.5–1 μm wide along a length of 40–100 μm.
3. Add microbeads (4.5 μm diameter, tosyl-activated) coated with integrin ligands, as described in *Protocol 2*, to cells (1–4 beads/cell) for 10–15 min. Beads should be bound to cells at this time, but not internalized.
4. Wash cells with cell culture medium to remove unbound beads. Transfer the coverslip onto the lid of 35 mm Petri dish filled with DMEM, and place it in the heated chamber (Omega RTD 0.1 stage heating ring at 37 °C) on the stage of an inverted microscope.
5. Position the tip of the uncoated glass micropipette alongside the surface-bound beads using the micromanipulator. Rapidly pull the bead away from the cell (about 5–10 μm/sec), parallel to dish surface.
6. Measure nuclear distortion, movement of the nuclear border, and any other cellular response to stress (e.g. redistribution of phase-dense organelles, such as mitochondria, vacuoles, or secretory granules) in the direction of the applied tension field using inverted phase-contrast, fluorescence, Nomarski, or birefringence microscopy in conjunction with real-time computerized image analysis (we use Oncor *Image Analysis* software).

Protocol 11. Analysis of stress transfer through the cytoskeleton

Equipment and reagents

- Nocodazole (10 μg/ml; Sigma), acrylamide (5 mM; Bio-Rad), or cytochalasin D (0.1–1 μg/ml; Sigma)
- Glass micropipette (0.5 μm diameter)
- See *Protocol 10*

Method

1. To analyse force transfer between the cytoskeleton and nucleus, 'harpoon' the cytoplasm with an uncoated glass micropipette (0.5 μm

Protocol 11. *Continued*

diameter) 10 μm from the nuclear border and then pull the pipette away, first 10 μm and then 20 μm at a rate of 5–10 μm/sec (*Figure 8*).

2. Culture cells in the presence of nocodazole (10 μg/ml), acrylamide (5 mM), or cytochalasin D (0.1–1 μg/ml) to disrupt or compromise microtubules, intermediate filaments, or microfilaments, respectively. Note: doses need to be adjusted for different cell types, and immunofluorescence staining should be carried out in parallel to ensure that the effects are specific and maximal.
3. Measure resultant changes in nuclear deformation induced by the 10 μm and 20 μm pulls simultaneously, using real-time video microscopy in conjunction with computerized image analysis, as described in *Protocol 10*.
4. Calculate nuclear strains in the direction of pull at 10 μm and 20 μm displacements. Nuclear movement is defined as displacement of the rear border of the nucleus in the direction of pull. Negative lateral nuclear strain (nuclear narrowing) is calculated by measuring changes in nuclear width perpendicular to the direction of pull.
5. To demonstrate direct connections between the cytoskeleton and nucleus, apply tension via a pipette placed closer to the nuclear border (2–4 μm). Note: if the cytoplasm pulls away from the nuclear border without deforming the nucleus or by causing it to narrow along its entire length (i.e. sausage-casing type effect), then the two structures are merely interposed with no connectivity. If stress application causes a small region of the nuclear envelope to protrude locally toward the pipette in the region of highest stress (*Figure 8*), then a direct connection must exist.
6. To demonstrate the presence of a distinct filamentous network within the nucleus, harpoon the nucleoplasm and pull inward. Local indentation of the nuclear border again indicates the presence of direct mechanical coupling at a localized site (*Figure 8*).

Protocol 12. Analysis of nuclear and cytoplasmic stiffness and connectivity

Equipment and reagents

- See *Protocols 10* and *11*

Method

1. To determine the ratio of nuclear to cytoplasmic stiffness, calculate strains in the direction of pull within regions of the nucleus and

cytoplasm located at the same distance from a pipette that is pulled 10 μm toward the cell periphery. This is accomplished by placing the pipette 5 μm or 10 μm from the nuclear border in two separate pulling experiments (i.e. in different cells under similar conditions).

2. When the pipette is placed 10 micrometers from the nuclear border, measure tip), in distal cytoplasm adjacent tot he nucleus (5-10 micrometers away), and in the proximal portion of the nucleus (10-15 micrometers away).

(10–15 μm away).

3. Perform identical measurements in similarly treated cells with a pipette placed 5 μm from the nuclear border to determine strains at the same distances (0–5, 5–10, or 10–15 μm) from the pipette tip and hence, under similar stress. These locations now fall in the cytoplasm adjacent to the nucleus, in the proximal nucleus, and in the distal nucleus, respectively (*Figure 9*).
4. Calculate the ratio of nuclear to cytoskeletal stiffness by determining the ratio of strains measured in the adjacent cytoplasm and proximal nucleus (i.e. 5–10 μm away from pipettes placed 10 μm and 5 μm away from the nuclear border, respectively), according to the equations described in *Figure 9*.
5. To measure apparent Poisson's ratios, harpoon the cells 10 μm from the nuclear envelope and pull the pipette 5 μm away from the nuclear border. Calculate the ratio of the strain (per cent changes in distances between different phase-dense particles in cytoplasm or nucleus) before and after stress application in the region along the axis perpendicular to the direction of pull divided by the strain in the direction of pull. All strains are measured in equal areas (9 μm^2), equally distant (4–5 μm) from both the pipette and the nuclear border, and all displacements should be of equal magnitude. Note: Poisson's ratio calculated in this manner must be viewed as an 'apparent' rather than absolute value, because the ratio is based on a two-dimensional projection of a three-dimensional material in cells adherent to an underlying solid substrate.

2.6 Analysing chromosomal connectivity and mechanics

Our work on mechanical connectivity in living cells suggested the existence of a continuous filamentous network within the nucleus as well as in the cytoplasm (37). To test directly whether discrete networks physically interlink chromatin in the nucleus, we used very fine glass microneedles (tips less than 0.5 μm diameter) to harpoon individual nucleoli within cultured interphase cells or individual chromosomes in mitotic cells. Using this approach, we found that pulling a single nucleolus or chromosome out from interphase or

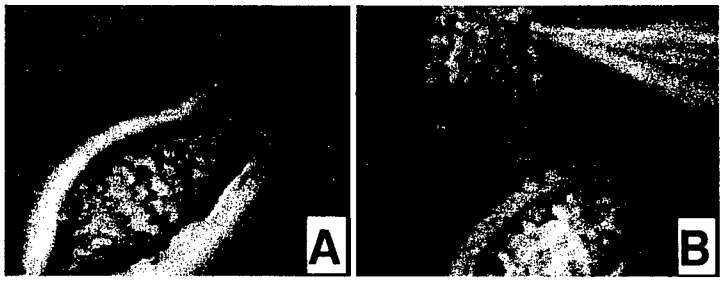

Figure 10. Microsurgical analysis of chromatin structure. A mitotic endothelial cell before (A) and after (B) a single chromosome was harpooned and removed from the cell using a micromanipulator. Note that pulling on one chromosome results in sequential removal of all the other chromosomes, revealing mechanical connectedness in the entire genome.

mitotic cells resulted in sequential removal of the remaining nucleoli and chromosomes, interconnected by a continuous elastic thread (40) (*Figure 10*). Enzymatic treatments of interphase nucleoplasm and chromosome chains held under tension revealed that mechanical continuity within the chromatin was mediated by DNA. Furthermore, when ion concentrations were raised and lowered, both the chromosomes and the interconnecting strands underwent multiple rounds of decondensation and recondensation (39–41). Fully decondensed chromatin strands also could be induced to recondense into chromosomes with pre-existing size, shape, number, and position by adding antibodies against histone H1 or topoisomerase II alpha, but not other nuclear proteins (39–40). These data suggest that DNA, its associated protein scaffolds, and surrounding cytoskeletal networks function as a structurally unified system. Mechanical coupling within the nucleoplasm may co-ordinate dynamic alterations in chromatin structure, guide chromosome movement, and ensure fidelity of mitosis. A typical assay is presented in *Protocol 13*.

Protocol 13. Analysis of chromatin mechanics and dynamics

Equipment and reagents

- See *Protocols 10* and *11*
- Glass coverslips
- Microscope
- 60 mM $MgCl_2$; trypsin; proteinase K

Method

1. Culture cells on glass coverslips in standard serum-containing medium. We have used endothelial cells and fibroblasts (39–41).
2. Transfer the coverslip to the lid of a 35 mm Petri dish covered with 2 ml serum-free medium with Hepes pH 7.4 and position on the stage of a Diaphot inverted microscope. For studies involving oil-immersion, use a cell culture chamber with a glass coverslip bottom, instead of 35 mm dish lid.

3. Fabricate the microneedle (0.5 μm wide tip), using methods in *Protocols 10* and *11*, and position it with the micromanipulator above a nucleolus or the edge of a mitotic plate.
4. Rapidly introduce the microneedle into the cell in a single motion and 'harpoon' an individual nucleolus or chromosome by gently touching it with the tip of the needle.
5. Pull out the nucleolus or chromosome attached to the microneedle through the original micropuncture opening made in the cell membrane by reversing the direction of pipette movement using the micromanipulator. The remaining chromatin strand will follow forming a continuous, elastic 'chain'. Note: the chromatin chain can be held in an extended form for study by either holding the micromanipulator in place or adhering the distal end of the chain to another cell or the surface of the culture dish by gently pressing the pipette against the surface. The connectivity between chromosomes can be studied by using the micropipette to apply a mechanical force directly to chromosome chains.
6. Probe the effect of different ions, chemicals, or biological compounds on chromatin mechanics and dynamics by placing a droplet (2 μl) containing the compound of interest directly above the isolated chain, or by replacing the original medium with the compound at the desired final concentration.
7. To analyse chromosome dynamics, incubate the extended chromosome chain with high salt, such as 60 mM $MgCl_2$ or place a 2 μl droplet of protease, such as the combination of trypsin (5 μg) and proteinase K (50 μg) above the isolated chain. The chromosomes will unfold and become phase lucent within seconds. These dynamic effects are reversible upon the return to the original ionic conditions or after addition of molecules involved in chromosome compaction (e.g. histone H1). Note: caution should be used during the handling of unfolded chromosomes, because excessive fluid turbulence can easily disrupt their pattern, entangle them, or cause non-specific sticking to the substrate. A more thorough description of methods and materials used to study chromosome dynamics *in situ* may be found in our recent publications (39–41).

3. Conclusion

In this chapter, we review a variety of different techniques that we have developed to manipulate and probe cell structure and cytoskeletal signalling. Our initial working hypothesis, based on a model of cellular tensegrity, suggested that cell form and function may be largely controlled based on

mechanical interactions between cells and their ECM. Our initial methods for varying cell–ECM interactions in a controlled manner were consistent with this model, because they showed tight coupling between cell spreading and growth. However, we could not discriminate signals triggered by cell shape modulation from signalling induced by local integrin receptor binding and clustering. In fact, by developing a microbead technique for inducing integrin clustering independently of cell spreading we could confirm that integrin binding alone is sufficient to activate many chemical signalling pathways that are involved in cellular control. Furthermore, we showed that much of this signalling occurs on the cytoskeleton at the site of integrin binding to the backbone of the FAC.

Nevertheless, when we finally developed a method to separate local cell–ECM binding events from cell spreading using micropatterned substrates, we discovered that cell shape exerts separate and distinct regulatory signals that act many hours after initial integrin and growth factor receptor signalling events to control cell cycle progression. In addition, we developed various other techniques to probe cell structure which revealed that the cell is indeed 'hard-wired' to respond to mechanical stresses; that cell surface adhesion receptors provide preferred sites for transmembrane mechanical transfer; and that living cells behave as if they are tensegrity structures when they are mechanically stressed. Taken together, these new methods have led to a new view of cell regulation based on tensegrity architecture in which mechanics and chemistry are tightly coupled. Better understanding of how cells control their shape and function will require development of more techniques that incorporate methods for controlling and quantitating changes in cell structure as well as biochemical events.

Acknowledgements

We would like to acknowledge the invaluable technical assistance of Deborah Flusberg, Adi Loebl, and Paul Kim, and thank Ruth L. Capella and Jeanne Nisbet for careful reading and editing of the manuscript. We would also like to thank Dr George Whitesides and the members of his group for their help in developing the micropatterning technique. This work was supported by grants from NIH, NASA, NSF, DOD, and NATO.

References

1. Ingber, D. E., Madri, J. A., and Jamieson, J. D. (1981). *Proc. Natl. Acad. Sci. USA*, **78**, 390.
2. Ingber, D. E. and Jamieson, J. D. (1985). In *Gene expression during normal and malignant differentiation* (ed. L. C. Andersson, C. G. Gahmberg, and P. Ekblom), p. 13. Academic Press, Orlando.
3. Ingber, D. E. (1993). *J. Cell Sci.*, **104**, 613.

4. Ingber, D. E. (1997). *Annu. Rev. Physiol.*, **59**, 575.
5. Ingber, D. E. (1998). *Sci. Am.*, **278**, 48.
6. Ingber, D. E. (1991). *Curr. Opin. Cell Biol.*, **3**, 841.
7. Ingber, D. E. (1993). *Cell*, **75**, 1249.
8. Ingber, D. E. (1990). *Proc. Natl. Acad. Sci. USA*, **87**, 3579.
9. Ingber, D. E. and Folkman, J. (1989). *J. Cell Biol.*, **109**, 317.
10. Mooney, D., Hansen, L., Farmer, S., Vacanti, J., Langer R., and Ingber, D. E. (1992). *J. Cell. Physiol.*, **151**, 497.
11. Lee, K.-M., Tsai, K., Wang, N., and Ingber, D. (1998). *Am. J. Physiol.*, **274**, H76.
12. Huang, S., Chen, C. S., and Ingber, D. E. (1998). *Mol. Biol. Cell*, **9**, 3179.
13. Folkman, J. and Moscona, A. (1978). *Nature*, **273**, 345.
14. Katz, B. Z. and Yamada, K. M. (1997). *Biochimie*, **79**, 467.
15. Schwartz, M. A., Lechene, C., and Ingber, D. E. (1991). *Proc. Natl. Acad. Sci. USA*, **88**, 7849.
16. Plopper, G. and Ingber, D. E. (1993). *Biochem. Biophys. Res. Commun.*, **193**, 571.
17. Plopper, G., McNamee, H., Dike, L. E., Bojanowski, K., and Ingber, D. E. (1995). *Mol. Biol. Cell*, **6**, 1349.
18. McNamee, H., Liley, H., and Ingber, D. E. (1996). *Exp. Cell Res.*, **224**, 116.
19. Miyamoto, S., Teramoto, H., Coso, O. A., Gutkind, J. S., Burbelo, P. D., Akiyama, S. K., *et al.* (1995). *J. Cell Biol.*, **131**, 791.
20. Burr, J. G., Dreyfuss, G., Penman, S., and Buchanan, J. M. (1980). *Proc. Natl. Acad. Sci. USA*, **77**, 3484.
21. Dike, L. E. and Ingber, D. E. (1996). *J. Cell Sci.*, **109**, 2855.
22. Xia, Y., Mrksich, M., Kim, E., and Whitesides, G. M. (1995). *J. Am. Chem. Soc.*, **117**, 9576.
23. Wilbur, J. L., Kim, E., Xia, Y., and Whitesides, G. M. (1995). *Adv. Mater.*, **7**, 649.
24. Singhvi, R., Kumar, A., Lopez, G. B., Stephanopoulos, G. N., Wang, D. I. C., Whitesides, G. M., *et al.* (1994). *Science*, **264**, 696.
25. Chen, C. S., Mrksich, M., Huang, S., Whitesides, G. M., and Ingber, D. E. (1997). *Science*, **276**, 1425.
26. Dike, L. E., Chen, C. S., Mrkisch, M., Tien, J., Whitesides, G., and Ingber, D. E. (1999). *In Vitro*, in press.
27. Wang, N., Butler, J. P., and Ingber, D. E. (1993). *Science*, **260**, 1124.
28. Wang, N. and Ingber, D. E. (1994). *Biophys. J.*, **66**, 2181.
29. Wang, N. and Ingber, D. E. (1995). *Biochem. Cell Biol.*, **73**, 327.
30. Wang, H. (1998). *Hypertension*, **32**, 162.
31. Potard, U. S., Butler, J. P., and Wang, N. (1997). *Am. J. Physiol.*, **272**, C1654.
32. Ezzell, R. M., Goldmann, W. H., Wang, N., Parasharama, N., and Ingber, D. E. (1997). *Exp. Cell Res.*, **231**, 14.
33. Goldmann, W. H., Galneder, R., Ludwig, M., Xu, W., Adamson, E. D., Wang, N., *et al.* (1998). *Exp. Cell Res.*, **239**, 235.
34. Yoshida, M., Westlin, W. F., Wang, N., Ingber, D. E., Rosenzweig, A., Resnick, N., *et al.* (1996). *J. Cell Biol.*, **133**, 445.
35. Pourati, J., Maniotis, A., Spiegel, D., Schaffer, J. L., Butler, J. P., Fredberg, J. J., *et al.* (1998). *Am. J. Physiol.*, **274**, C1283.
36. Chicurel, M. E., Singer, R. H., Meyer, C. J., and Ingber, D. E. (1998). *Nature*, **392**, 730.

37. Maniotis, A. J., Chen, C. S., and Ingber, D. E. (1997). *Proc. Natl. Acad. Sci. USA*, **94**, 849.
38. Eckes, B., Dogic, D., Colucci-Guyon, E., Wang, N., Maniotis, A. J., Ingber, D., *et al.* (1998). *J. Cell Sci.*, **111**, 1897.
39. Maniotis, A. J., Bojanowski, K., and Ingber, D. E. (1997). *J. Cell Biochem.*, **65**, 114.
40. Bojanowski, K., Maniotis, A. J., Plisov, S., Larsen, A. K., and Ingber, D. E. (1998). *J. Cell Biochem.*, **69**, 127.
41. Bojanowski, K. and Ingber, D. E. (1998). *Exp. Cell Res.*, **244**, 286.

...cells show greater fragmentation. These results demonstrate that intravasation is a rate-limiting step in the process of metastasis and that cell-based assays for determination of cell properties in vivo are necessary for dissection of the metastatic process.

...conditioned endothelial media failed to stimulate chemotaxis of the non-metastatic WM35 cells. Migrating WM239 cells sent out fan-shaped lamellipodia in the direction of the conditioned media. Immunofluorescence labeling showed an abundance of $\alpha v\beta 3$ integrin and actin filaments associated with the leading edges. Chemotaxis of WM239 cells was abrogated when either tubulin or actin filaments were disrupted using latrunculin B or cytochalasin D. Taken together, the data demonstrate that endothelial cells secrete specific chemoattractants which may play a role in tumor metastasis. (Supported by the Medical Research Council of Canada.)

1516

METAL ANTAGONISTS OF RESTING CALCIUM INFLUX PATHWAYS INHIBIT THE MOTILITY OF B16F10 MELANOMA CELLS.

C.G. Carlson , T. Lancaster, and J.L. Cox. Depts. of Physiology and Biochemistry, Kirksville College Osteopathic Medicine, Kirksville, MO 63501.

Cell attached and inside-out patch clamp recordings from B16F10 melanoma cells, obtained at elevated and normal Ca^{2+} concentrations, indicated the presence of nonselective cation channel activity and calcium selective activity that increased as the membrane potential was hyperpolarized below resting potential. Fluorimetric Mn^{2+} - quench determinations using FURA loaded cells also indicated resting Ca^{2+} influx that is blocked by the lanthanides. These results provide electrophysiological and fluorimetric identification of resting Ca^{2+} influx pathways in a highly metastatic cell line. To determine whether such pathways are involved in the motility of these cells, we examined the effects of metal antagonists (2 mM $CoCl_2$, 20 μM $GdCl_3$) of resting Ca^{2+} influx pathways on B16F10 motility (bFGF stimulated, Boyden chamber assay) at normal, reduced, and elevated K^+ concentrations. Motility was highly dependent upon the K^+ concentration and increased between 250 to 290% at low (0.54 mM) and elevated (54 mM) K^+ concentrations. $GdCl_3$ and/or $CoCl_2$ markedly and consistently inhibited (between 70 and 95%) motility at normal, reduced, and elevated K^+ concentrations. In contrast, verapamil (100 μM) produced only marginal reductions in motility. These results strongly suggest that resting Ca^{2+} influx, through pathways that have been identified in B16F10 melanoma cells, is essential to the movement of metastatic cells, and that metal and other antagonists of such pathways may be useful in the treatment of a variety of highly metastatic cancers.

1517

ROLE OF INTEGRIN RECEPTORS IN VASCULAR SMOOTH MUSCLE CELLS MIGRATION ON INTACT AND DEGRADED EXTRACELLULAR MATRIX.

Emanuela Stringa, Gillian Murphy, Jelena Gavrilovic, University of East Anglia, Norwich, Norfolk NR4 7TJ

Vascular smooth muscle cells (VSMC) are normally found in the tunica media of arteries and veins. During atherosclerotic plaque development, VSMC lose contractility and migrate from the tunica media to the intima through basement membrane and interstitial collagenous matrix. The role of VSMC migration on degraded ECM was evaluated. We previously showed that umbilical artery SMC adhere to native intact collagen type I and to its ¾ fragment (generated by collagenase-3 cleavage) unwound at 35°C to mimic physiological conditions. Moreover, PDGF-BB treatment induced a 2-fold increment in VSMC motility on unwound ¾ fragment. On the contrary, PDGF-BB did not induce a significant change in VSMC motility on collagen type I. The integrin alpha2beta1 is responsible for motility on collagen type I: inhibition of VSMC motility was obtained using a monoclonal antibody against alpha2. VSMC motility on unwound ¾ fragment was abolished using LM609, a monoclonal blocking antibody versus alphavbeta3. This integrin receptor is organized in focal adhesions and co-localized with vinculin and focal adhesion kinase. The role of PDGF receptor beta on VSMC motility on intact and degraded collagen type I is under investigation. These results implicate potential integrin-growth factor receptor cross-talk in the migration of VSMC over degraded collagen. (Supported by the British Heart Foundation, Grant no. PG97040).

8

...omic Analysis of Tumor Metastasis

...n A Clark[1], Todd Golub[2], Richard O Hynes[1], [1]Massachusetts Institute of Technology, 77 ...achusetts Ave, Cambridge, MA 02139, [2]Whitehead Center for Genomic Research

...most feared aspect of cancer is its ability to spread throughout the body, or metastasize, ...t is this dissemination of tumorigenic cells that is the principal cause of death from ...r. The progression of tumorigenic cells from benign growths to metastatic malignancies ...een suggested to be caused by a change in expression of specific genes whose protein ...cts regulate the malignant state. Therefore, we were interested in identifying genes ...e expression consistently changes in parallel with tumor progression. We have taken a ...ic approach to identifying "metastasis genes" using gene expression microarrays. ...r samples are derived from poorly metastatic melanoma cell line (human A375P and ...B16F0) grown subcutaneously, and compared to pulmonary metastases of these cell ...njected intravenously. A total of 31 genes show enhanced expression (at least 2.5-fold ...) in all metastases examined. The role of these genes in metastasis is currently being ...by using retroviral vectors to express dominant-inhibitory versions of these genes (or ...se constructs) in the metastatic cells and subjecting them to both *in vitro* and *in vivo* ...asis assays.

1519

Application of an automated, high-throughput assay to identify perillyl alcohol as a non-cytotoxic inhibitor of breast cancer cell migration

Johanna E. Wagner[1], Carla DiGennaro[1], J. Abiodun Elegbede[1], Will Rust[1], George E. Plopper[2], [1]University of Nevada at Las Vegas, 4505 Maryland Parkway, Las Vegas, NV 89154-4004, [2]University of Nevada, Las Vegas

Most anti-cancer drugs developed thus far target hyperproliferation of metastatic cells and many have cytotoxic properties that cause deleterious side effects. Because cell migration plays a central role in the metastatic cascade, it is an attractive target for novel anti-cancer drug design. Current techniques for measuring cell migration are labor-intensive and costly and therefore, limit the rate of drug screening and discovery. We developed an automated, high-throughput migration/cytotoxicity assay and used it to screen for non-cytotoxic inhibitors of cancer cell migration. This assay revealed that perillyl alcohol, an experimental anti-tumor drug, retards migration of MDA-MB 435 breast cancer cells on fibronectin in an 18-hour assay at non-cytotoxic (>60% viability) and clinically efficacious doses. 10 mM sodium butyrate, which induces apoptosis in these cells, fails to inhibit migration in this assay. This effect of perillyl alcohol is dose-dependent up to 2.0 mM and does not alter cell adhesion to extracellular matrix proteins. However, the same concentrations of perillyl alcohol do not affect migration or viability of immortalized, non-tumorigenic (MCF-10A) breast cells. Because its anti-migratory effects are distinct from its cytotoxic effects, perillyl alcohol serves as a model for identification of new non-cytotoxic drugs that specifically target cell migration.

epithelial cell. Adhesion to fibronectin, but not to laminin, is sufficient to transiently upregulate the levels of c-Myc protein in quiescent epithelial cells in a fibronectin concentration-dependent manner. Full activation of c-Myc expression by fibronectin requires an intact actin cytoskeleton. Furthermore, this c-Myc upregulation requires integrin aggregation, since c-Myc can be induced in suspension culture by fibronectin-coated microbeads, but not by soluble fibronectin. In addition, the increase of c-Myc following adhesion to fibronectin can be impeded by addition of a blocking antibody against the β1 integrin subunit, directly implicating β1 integrins in the control of c-Myc expression. Fibronectin regulation of c-Myc does not involve the MAP kinase pathway previously implicated in integrin regulation of G1 phase progression, since the specific inhibitor of MEK1, PD98059, does not alter the level c-Myc in cells spread onto fibronectin. These results show that adhesion of mammary epithelial cells to the extracellular matrix through β1 integrins plays a direct role in c-Myc upregulation.

neuronal cell lines including PC12 cells. Identification of neurite ou laminin domains has been made possible, in part, through the used of which are derived from laminin sequences. Recently a synthetic peptide with the amino acid sequence RKRLQVQLISRT was shown to stimulate n PC12 cells. Here we tested the ability of laminin and the AG-73 peptid production in PC12 cells. We found that laminin stimulates nitric oxide p dependant manner. Further, the AG-73 peptide also stimulated nitric oxi additional laminin-derived synthetic peptide, designated C16, which p attachment, but not neurite outgrowth, was also tested for the ability to sti production. The C16 peptide did not activate PC12 cell nitric oxide produc the ability of laminin and the AG-73 peptide to stimulate nitric oxide pro the promotion of neurite outgrowth. Preliminary data suggest that the ni inhibitor, l-name, blocks laminin mediated neurite outgrowth. Taken to that laminin activates nitric oxide production in neuronal cells and that required in the mechanism of laminin-mediated neurite outgrowth.

1961

Assessing the Contributions of Lipoxygenases in HeLa Cell Spreading.

Louis Anthony Roberts, Bruce S. Jacobson, University of Massachusetts, 913 Lederle GRC, Amherst, MA 01003

Integrin-mediated adhesion of cells to an extracellular matrix (ECM) and subsequent cell migration have been implicated in the biologically important processes of wound healing, metastasis, and angiogenesis. Arachidonic acid (AA) is released from membrane phospholipids by cytosolic phospholipase A_2 (cPLA$_2$) upon HeLa cell adhesion to collagen. AA is metabolized to leukotrienes (LTs) and hydroxyeicosatetraenoic acids (HETEs) by the lipoxygenase (LOX) pathway, which leads to cell spreading. Three branches of the LOX pathway have been identified which may contribute to HeLa spreading, with the 5, 12, and 15LOX enzymes catalyzing the initial divergent steps of LOX metabolism of AA. We are currently investigating the roles of these LOX enzymes in HeLa spreading by assessing the relative contributions of each in the spreading process. Using constitutive and inducible overexpression of these enzymes in conjunction with pharmacological inhibition, we have determined that 5LOX contributes to HeLa spreading on collagen. Our results also suggest that 12LOX may not be involved in the spreading process. Studies with 15LOX are in progress. We are also assessing changes in cell phenotypes (spreading/migration kinetics, actin polymerization/bundling, LOX/COX metabolites levels) upon induction/inhibition of the LOX enzymes. The results obtained in these studies can provide the basis to investigate other AA-mediated cell processes, such as angiogenesis.

1962

Macrophages Adherent to Matrices Containing Thrombospondin-1 Se

Jens Husemann, Samuel C Silverstein, Columbia University, 630 West York City, NY 10032

Human monocyte-derived macrophages (Macs), 4-6 days in culture, containing acetylated- or oxidized-low density lipoproteins (acLDL or oxl A scavenger receptors (SR-A). Macs secrete H_2O_2 when they adhere surfaces, but not to acLDL-coated surfaces. Antibodies that block CD36, receptor, have no effect on Mac adhesion to surfaces containing acLDL o H_2O_2 production by cells adherent to oxLDL-coated surfaces by ~50% *Exp. Med.* 188:2257,1998). We report here that Macs adherent to su thrombospondin-1 (TSP-1), a physiological ligand for CD36, secrete ~40 Macs plated on oxLDL-coated surfaces, and that Macs adherent to surfac TSP-1 and acLDL secrete nearly as much H_2O_2 as Macs adherent to oxLI The presence of TSP-1 in the medium did not inhibit H_2O_2 secretion b Macs. These results suggest that cross-linking of CD36 by matrix-associ H_2O_2 secretion by Macs, and that matrices that cross-link CD36 in combi scavenger receptors provide a stronger stimulus for Mac H_2O_2 secretion cross-link CD36 alone.

1963

Stimulation of breast cell migration on laminin-5 by antibody induced activation of α3β1 integrin receptor and a Gαi3-mediated signaling pathway

Kilpatrick J. Carroll[1], Vincent J. Cavaretta[1], Russell W. Bandle[1], Janice L. Huff[1], Martin Alexander Schwartz[2], Vito Quaranta[2], George E. Plopper[1], [1]University of Nevada Las Vegas, 4505 Maryland Parkway, Las Vegas, NV 89154-4004, [2]The Scripps Research Institute

We have recently shown that malignant breast cells constitutively migrate on laminin-5, a component of breast basement membrane, while normal and immortalized (non-malignant) breast cells do not. In this study we focused on identifying signaling pathways that control migration in these cells. We report that direct stimulation of the α3β1 integrin receptor with the β1 stimulating antibody TS2/16 was sufficient to induce haptotactic migration of the immortalized, non-malignant breast cell line MCF-10A on laminin-5, but not on laminin-1. TS2/16-stimulation also induced a rapid rise in intracellular cyclic AMP within 20 minutes after these cells were plated on laminin-5. Pertussis toxin (PTX) inhibited both haptotactic migration and the rise in cyclic AMP levels in TS2/16-stimulated cells. The Gαi3 subunit of heterotrimeric G proteins was identified as the target of PTX in immunoprecipitates of ADP-ribosylated proteins following PTX exposure. TS2/16-stimulated migration on laminin-5 was also blocked by inhibitors of adenylate cyclase (SQ22536) and protein kinase A (H-89), suggesting that these signaling proteins may form an integrin-associated, Gαi3-linked signaling pathway in MCF-10A cells.

1964

Extracellular matrix-cell communication: Plant cell wall-associated kin

Mireille C. Perret, Tanya A. Wagner, Cathy Anderson, Bruce D. Kohorn Research Drive, Durham, North Carolina 27708

The plant extracellular matrix is a meshwork of carbohydrates and prc structural role in shaping and supporting the plant cell and mediates sigr extracellular space and the cytoplasm. The receptor-like wall associated k in *Arabidopsis thaliana* are good candidates for performing a signaling rc an extracellular domain attached to the cell wall and an intracellular serir domain. The divergence in the amino acid sequence of the extracellular do tissue expression on Northern blots suggests that the five Waks may have Genetic analysis, including gene disruption, promoter fusions, overexpress indicates that the Waks are involved in development and cell expansion, distinct patterns of expression and induction. Potential ligands for the extra several of the Waks have also been found.